Journal of African Earth Sciences 108 (2015) 74–88

Contents lists available at ScienceDirect

Journal of African Earth Sciences

journal homepage: www.elsevier.com/locate/jafrearsci

The effects of extensional structures on the heat transport mechanism: An example from the Ortakçı geothermal field (Büyük Menderes Graben, SW Turkey)

Ali Kaya *

Pamukkale University, Faculty of Engineering, Department of Geological Engineering, 20017 Kınıklı, Denizli, Turkey

ARTICLE INFO

Article history:
Received 25 March 2015
Received in revised form 21 April 2015
Accepted 5 May 2015
Available online 14 May 2015

Keywords:
Structural controls
Extensional tectonics
Active faulting
Büyük Menderes graben
Heat transport mechanism
Relay ramp

ABSTRACT

The extensional stress regime is very effective in western Turkey since the Latest Oligocene-Early Miocene. Geothermal fields are positioned on the high-angle normal faults along the northern and southern margins of the Büyük Menderes and Gediz grabens, respectively. The Ortakçı geothermal field is located on the tectonically active northern margin of Büyük Menderes graben. The discharge rate and temperature of the Ortakçı hot spring is 2.4 l/s and 50.5 °C, respectively. Hot water discharges in the relay ramp representing the overlapping regions of two E–W normal faults related to N–S-oriented extension. The high-angle normal faults provide pathways for the fluid flow by increasing dilations. The field observations prove that all hot water outflows are related to the high-angle normal faults on the hanging wall of the detachment faults. Detailed structural analyses were performed on the Ortakçı geothermal field, particularly on one of the active hot springs at the intersection of the E–W and N–S-oriented faults, to evaluate the tectonic activity in the area and the flow pathways for geothermal fluids. The heat source is the shallow mantle of a thinned lithosphere due to large extension rates, resulting in increased heat flow. The tectonic effects are on the heat transport mechanism, and the heat transport is controlled by faults in a convection dominated systems. The result is a high geothermal gradient because water can circulate deep and transports the heat upwards to the surface.

1. Introduction

Obvious relationships exist between geothermal systems and structural elements in which active hydrothermal outflows are present (Curewitz and Karson, 1997). Faults and fractures play a major role in flow path orientation, localization and the evolution of hydrothermal fluids (e.g. Norton and Knapp, 1977; Kerrich, 1986). Deeply penetrating faults typically provide pathways for geothermal fluids within the crust and are therefore the primary means for efficient heat transfer from deep to shallow crust levels in amagmatic regions (Faulds et al., 2009).

The study area is located in the Büyük Menderes graben, in western Turkey (Fig. 1). Western Turkey is an actively deforming section of the Aegean extensional province and comprises one of the highest rate deforming areas of the Alpine-Himalayan mountain belt (Dewey and Şengör, 1979; Jackson, 1994). In western Turkey, the roughly north–south extension (~30–60 mm/yr) has resulted in approximately E–W oriented graben systems (Jackson and McKenzie, 1988). Northeast directed transverse faults dissect the northern margin of the graben and commonly extend into the Menderes massif (Şengör, 1987).

The Ortakçı relay ramp is one such feature in the study area. It is located at the eastern end of the Büyük Menderes Graben which is approximately 165 km long and 2–16 km in width. The graben narrows up to 2 km at the Kızıldere field, where it bends towards the south-east. Similarly, the Germencik geothermal field bends towards the south-west (Fig. 1). The thermal water of the Ortakçı relay ramp is situated between two active normal fault segments having the same dip direction.

The geological development of the eastern Mediterranean and its surrounding regions has been primarily controlled by the roll-back of the subduction of the African lithosphere beneath the Hellenic and Cyprus trenches (Fig. 1; Le Pichon and Angelier, 1981; Taymaz et al., 1991; Reilinger et al., 2006). Researchers have proposed several models for the current extensional tectonics regime in western Turkey. The best-known models are *tectonic escape* (Dewey and Şengör, 1979; Şengör, 1982), *back-arc spreading* (McKenzie, 1978; Le Pichon and Angelier, 1981; Jackson and McKenzie, 1988; Reilinger et al., 2006), *orogenic collapse* (Dewey,

* Tel.: +90 258 2963376; fax: +90 258 2963460.
E-mail address: alikaya@pau.edu.tr

http://dx.doi.org/10.1016/j.jafrearsci.2015.05.002
1464-343X/

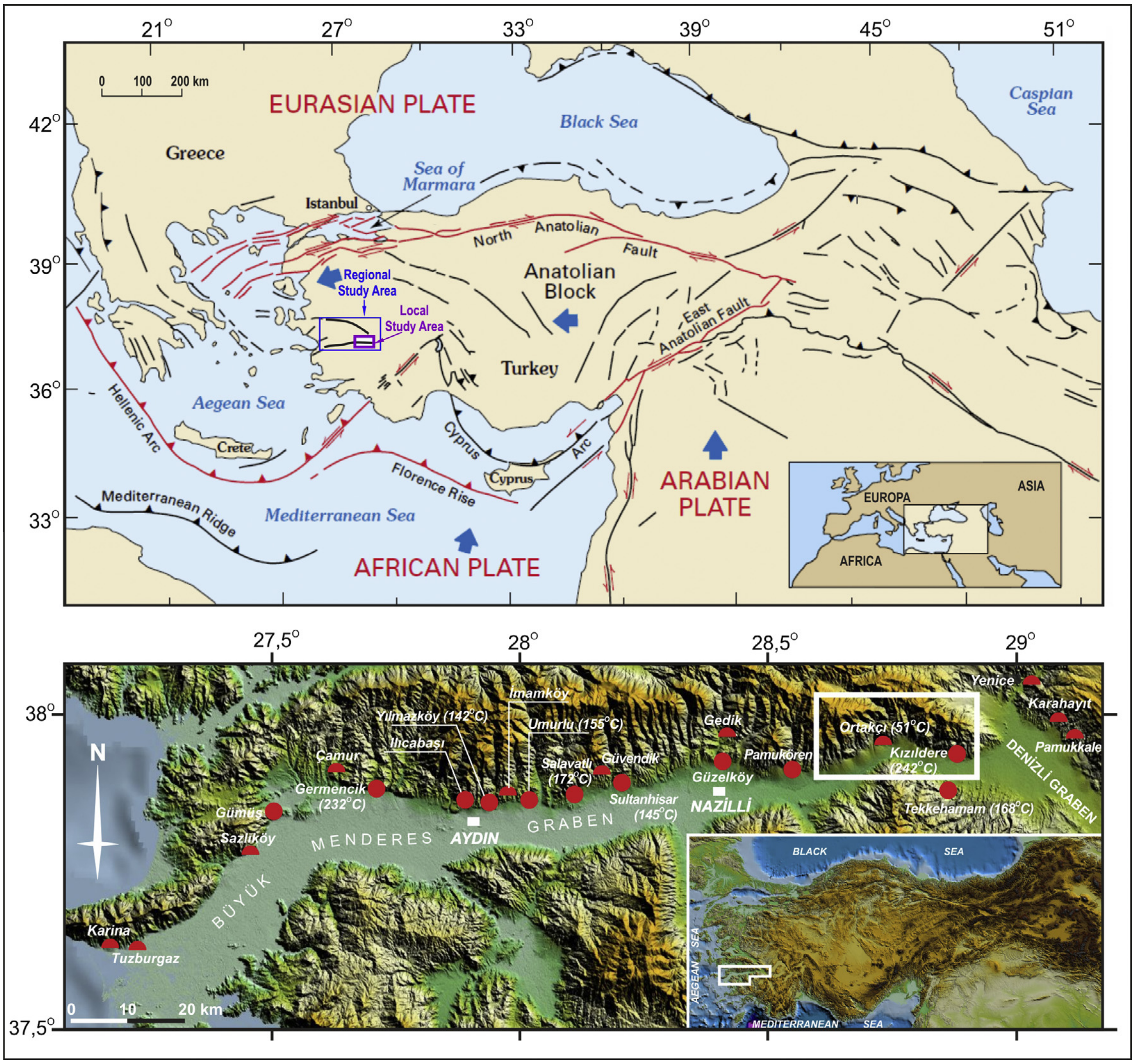

Fig. 1. Tectonic map of Turkey (modified from USGS, above), location map of the study area and the distribution of geothermal fields in the Büyük Menderes graben, the fields from Karakuş and Şimşek (2013). The spheres and semi-spheres represent the locations of deep geothermal wells and hot springs, respectively (below).

1988; Seyitoğlu and Scott, 1991, 1996) and *episodic two-stage graben* (Koçyiğit et al., 1999; Koçyiğit, 2005; Bozkurt, 2000; Bozkurt and Sözbilir, 2004; Bozkurt and Rojay, 2005).

The nature of the heat source for the geothermal systems of western Anatolia is up for debate. Because of its active extensional deformation setting, western Anatolia has significant potential for geothermal energy resource discovery. The Büyük Menderes graben, consisting of typical high enthalpy geothermal fields (Kızıldere, Salavatli and Germencik; Fig. 1), has significant potential of new geothermal field discover, in addition to the location of a number of well-known fields. Although some existing models of the geothermal field heat source in the study area suggest a probable magmatic intrusion (e.g. Şimşek, 1985), no evidence exists for the presence of a present-day magmatic activity. The heat source for the waters of the Menderes graben has been associated with young tectonic activity resulting from the absence of magmatic activity in the region (e.g. Faulds et al., 2009). The present study aimed at determining the relationships between the structural controls and the Ortakçı hot spring. Detailed geologic maps, structural analysis of the area's faults and the surface geothermal features in the region were studied. An analysis of structural data from tectonically active areas may be useful for the exploration of potential geothermal fields.

2. Geological setting

The E–W striking Büyük Menderes graben is 165 km long (Figs. 1 and 2). A major south-dipping normal fault system bounds the northern margin of the graben. The total vertical displacement of the normal faults within the system is estimated minimum 1 km based on field observations and geothermal borehole data. The normal faults juxtapose Neogene and Quaternary sedimentary units against the metamorphics Menderes massif (Figs. 2 and 3). Many hot springs are located along the normal fault zones of the graben (e.g. Şimşek, 2003; Fig. 1).

The study area is part of the Büyük Menderes graben that forms southern boundary of the Central Menderes massif (CMM, Fig. 2). The Menderes massif covers a large area of western Turkey, and consists of quartz-muscovite schist, biotite-quartz schist, garnet micaschist and augen gneiss (biotite gneiss and pegmatitic gneiss). Augen gneisses (orthogneisses) are metagranites that intrusive in schists. Pb–Pb single zircon age has yielded 551 ± 1.4 Ma from the granitic Birgi augen gneisses in the Ödemiş-Kiraz submassif (Hetzel et al., 1998). Detrital zircon ages at about 550 Ma in the Paleozoic muscovite-quartz schists show that these Pan-African granitoids in the basement form the source rocks of the cover series of the Menderes massif (Koralay et al., 2012). Furthermore,

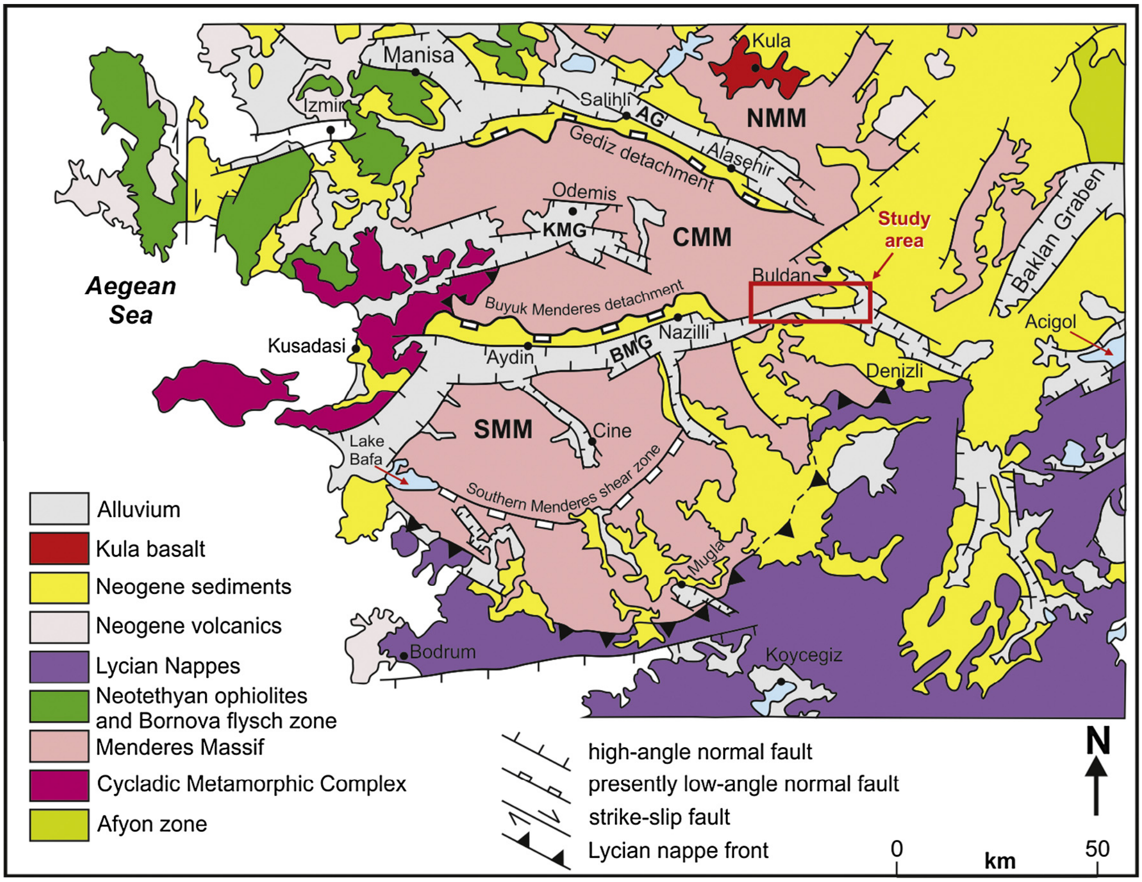

Fig. 2. Geological map of western Turkey showing the Menderes massif and its subdivision into the AG Alasehir graben, the BMG Büyük Menderes graben, the CMM Central Menderes massif, the KMG Küçük Menderes graben, the NMM Northern Menderes massif and the SMM Southern Menderes massif, modified from Şengör and Bozkurt (2013).

massive intercalated amphibolites and amphibolite schists are present. These rocks may have been metamorphosed into paragneiss during the first metamorphism phase in the Cambrian-Ordovician (Dora et al., 1990; Dora, 2011; Hetzel and Reischmann, 1996). The second main metamorphism phase of the massif is associated with the emplacement of the Lycian nappes onto the Menderes massif in the Paleocene-Late Eocene (Şengör and Yılmaz, 1981; Şengör et al., 1984; Bozkurt, 2000; Rimmele et al., 2003).

The Neogene sequents in the study area are covered by Quaternary colluvium and alluvium and they are exposed in other parts of the graben. The thickness of Miocene and Pliocene sedimentary units reaches up to 1950 m based on borehole data in the Sarayköy (Gerali) geothermal field at the eastern end of the Büyük Menderes Graben (Karamanderesi and Ölçenoğlu, 2005). Pliocene fluvial and lacustrine sediments are about 1400 m in thickness (Şimşek et al., 2005). Miocene-Quaternary sedimentary units are only 700 m in Germencik geothermal field at the western end of the graben (Karamanderesi, 2013). It means that the graben is getting deeper from west to east. The oldest unit in the graben is a clastic succession associated with lacustrine limestone of Early Miocene (Kazancı et al., 2009).

The geological development of the region resulted from the convergence between the African and Eurasian plates, which has included subduction, orogenesis, crustal extension and large-scale strike-slip faulting. Turkey, which is located in the Alpine-Himalayan orogenic belt, has experienced compressional and extensional tectonics during the paleotectonic and neotectonic periods, respectively, associated with the evolution of the Tethys.

Western Turkey has undergone significant approximately N–S neotectonic extension, reaching 20 mm/yr (Reilinger et al., 2006), this value is correspond to a deformation rate approximately 65 nano-strain/yr. The timing of the initiation of this extension is a controversial and varies among studies from Early Oligocene (Sözbilir, 2005), Late Oligocene-Early Miocene (Seyitoğlu et al., 1992, 2002; Işık et al., 2003; Purvis and Robertson, 2004), Early Miocene (Kazancı et al., 2009), Late Miocene (Lips et al., 2001) to Pliocene–Pleistocene (e.g. Koçyiğit et al., 1999; Bozkurt, 2000; Yılmaz et al., 2000).

The central Menderes massif core-complex which has exhumated on the footwalls of south facing of Büyük Menderes detachment and north facing of Gediz detachment in the south and in the north respectively (Hetzel et al., 1995; Gessner et al., 2001; Gürer et al., 2009). The most prominent fault is Büyük Menderes Detachment Fault in the graben. In addition to these approximately E–W running normal faults, NW–SE, NE–SW and N–S oriented fault systems have also been found (Fig. 3).

The study area, reflects earlier compressional and subsequent extensional deformation events during the pre-Oligocene and Latest Oligocene-present day periods, respectively. The compressional deformation events caused crustal shortening and were associated with E–W trending folds, thrust faults, nappes sutures and contemporaneous metamorphism. The subsequent extensional tectonic regime (Neotectonic regime sensu strictu) began in the Late Oligocene age (Angelier et al., 1982; Seyitoğlu et al., 1992; Gessner et al., 2001) resulted in the extensional exhumation of metamorphic rocks of the Menderes massif, in a classical core complex scenario (Davis, 1983; Wernicke, 1985; Lister and Davis,

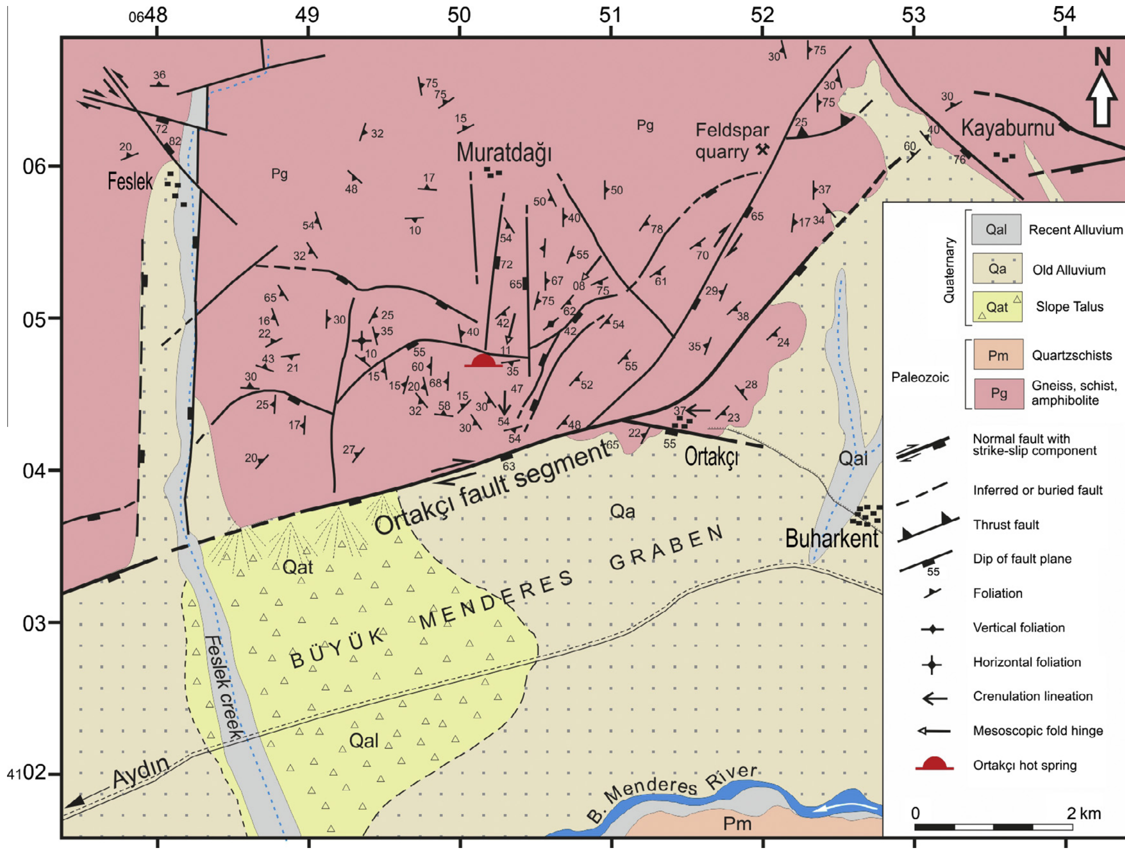

Fig. 3. Detailed geological map of the Ortakçı thermal spring area (Buharkent-Aydın).

1989). The dominant feature of the deformation in the Aegean region from this period onward has been extensional motions combined with strike-slip motions (Jackson, 1994).

2.1. Compressional structures

The Menderes massif has been subjected to polyphase deformation and greenschist to amphibolite facies metamorphism. Three phases of folding are recognised in the area. Fig. 4 demonstrates that S_1 foliation planes (formed during the D_1) deformed at least twice. The planar and linear structures of the region are associated with the F_1, F_2 and F_3 folding events. The D_1 deformation phase includes bedding-parallel ductile shear zones, F_1 mesoscopic folds and S_1 foliation. Further shortening during the D_2 phase, deformed S_1 foliation surfaces and created WNW–ESE oriented inclined F_2 folds in the study area (Fig. 4). Continued crustal shortening during the third-phase resulted in upright macroscopic F_3 folding and S_3 cleavage development and L_3 lineation (crenulation and mesoscopic fold hinge). During the F_3-phase, crustal shortening produced Type-2 interference fold patterns, which can generally be observed in outcrops associated with S_3 crenulation cleavage (Fig. 4).

The type 2-fold patterns produced by the superposition of a non-coaxial third upright fold set upon an inclined second-phase fold pattern. The mushroom style patterns on the horizontal plane (Fig. 4) indicate two compressional directions perpendicular to each other. The fold axial traces (F_2, F_3; Fig. 4) and contour diagrams (Fig. 5a and b) of schistosity and lineation measurements also support the presence of at least three deformation phases. The second deformation phase, D_2, is WNW–ESE oriented, whereas the third deformation phase, D_3, is NNE–SSW oriented. The NNE–SSW direction D_3 deformation phase in particular is thought to have been formed by strong folding (Figs. 4 and 5).

2.2. Extensional structures

The neotectonic structures are related to brittle tectonics and dominated by normal or normal-oblique-slip faults, resulting in horst and graben structures. Along the graben-bordering normal faults, the metamorphic rocks in the footwall have been lifted 1 to 2 km. A vertical total throw of 2080 m in the Miocene sequence was measured on the normal faults of the southern margin of the basin near Sarayköy by Koçyiğit (2005), whereas it is approximately 1300 m in Kızıldere geothermal field, based on the geothermal borehole data (Şimşek, 1985). The N–S extension in the Büyük Menderes graben has caused E–W, NW–SE and NE–SW oblique striking normal faults, with dip values of 50–70° (Figs. 2 and 6). The region is also dissected by many N–S trending strike-slip faults serving as lateral ramps.

NW–SE and NE–SW trending conjugate pairs of oblique striking normal faults, which are E–W extension related to N–S contraction and transpression, are associated with the earlier tectonic events in the Early-Middle Miocene. Whereas, roughly E–W trending high-angle normal faults and E–W directed Büyük Menderes Detachment Fault (BMDF) are related to subsequent N–S extension tectonic events (Gürer et al., 2009).

The exhumation of central Menderes metamorphic core complex is bivergent continental breakaway zone in the western Turkey (Gessner et al., 2001). It has started to form along the north of Alaşehir and south of Büyük Menderes grabens in the Latest Oligocene-Early Miocene (Seyitoğlu and Scott, 1991; Hetzel et al., 1995; Gessner et al., 2001; Catlos and Çemen, 2005; Van Hinsbergen et al., 2010). The Menderes massif was exposed the

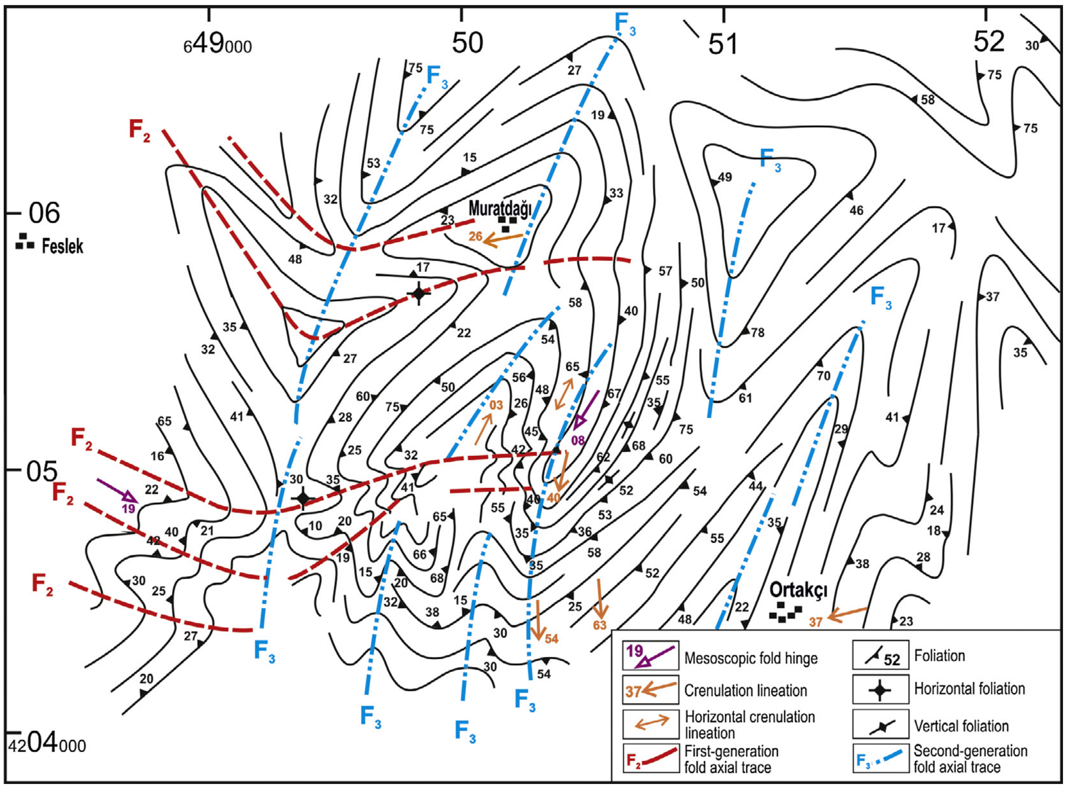

Fig. 4. Structural map of the study area showing the mesoscopic planar and linear elements and traces of foliation surfaces associated with F_1, F_2 and F_3 folding events.

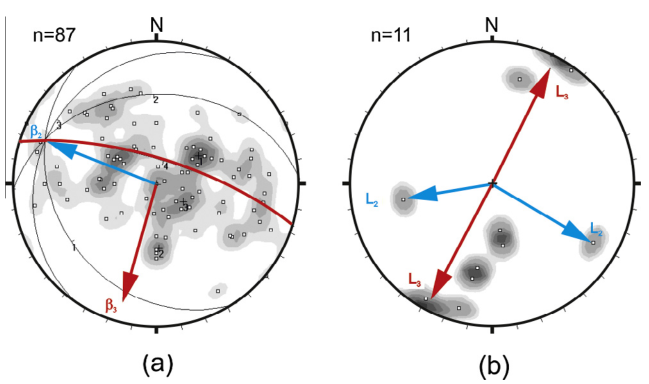

Fig. 5. Lower hemisphere equal area stereographic plots of mesoscopic data from the Ortakçı geothermal area. (a) Stereographic plots of the foliation planes (b) poles of mylonitic and gneissic foliation planes and (a) where blue arrow and β_2 are fold axis related to second generation folding, red arrow and β_3 are fold axis related to third generation folding; L_2 and L_3 are crenulation lineations (b).

Early Miocene tectonic denudation and surface uplift in the footwall of a north-directed extensional detachment system, followed by the Late Miocene to recent fragmentation by E–W and NW–SE trending graben systems (Gessner et al., 2013).

Büyük Menderes detachment fault is commonly S-dipping with a small right-lateral strike-slip component. Dip values vary from 40° to 65°. It is running along the northern margin of the Büyük Menderes Graben, and is approximately E–W directed (Fig. 2). The fault surface of the BMDF shows both ductile and brittle deformation features, (Gürer et al., 2009; Hetzel et al., 1995; Gessner et al., 2001). Along the southern margin of the Alaşehir graben, Gediz detachment fault is generally N-dipping with dips ranging between 15° and 20°. Hanging walls of the both detachment faults are cut by E–W directed high-angle normal faults along the southern margin of the Alaşehir graben and northern margin of the Menderes graben (Gessner et al., 2001; Işık et al., 2003; Bozkurt, 2003).

The existence of thick and widespread scree deposits in front of the faults on the northern margin of the Büyük Menderes graben indicates that these faults are experienced larger displacement rates and are more active than those to the south (see Figs. 2 and 3). The continuous movements of the colluvium deposits to the south have displaced the Büyük Menderes River towards the south (Fig. 2). In addition, the presence of the hot springs in the northern segment of the graben suggests that this area is currently active.

The northern margin of the graben is bounded by a mainly south-dipping normal fault system with a strike-slip component of motion. These approximately E–W striking faults have vertical offset of at least approximately 1 km. The Neogene sediments are juxtaposed with the Menderes massif metamorphic units along these faults. The most obvious fault segments associated with the Ortakçı thermal spring are the Ortakçı, Çatak-Sazak and Kızıldere segments, all of which are roughly E–W trending. The ENE–WSW trending Ortakçı fault segment is an approximately 17 km long normal fault, with a right-lateral strike-slip component. The morphological signature of scarps along this fault proves suggests a vertical throw of approximately 600 m. This fault forms the border of the Menderes metamorphic rock and alluvial deposits (Fig. 3).

The NW–SE to E–W trending Çatak-Sazak fault segment is an approximately 20 km long normal fault with a right-lateral strike component and is located between Çatak village to the west and Sazak village to the east (Fig. 6). The fault breaks into multiple splays (or horsetail splays) at its western end, near Muratdağı (Figs. 2 and 6). Based on the fault's scarps at the north of the Kızıldere geothermal power plant, its throw is at approximately 300 m. The Kızıldere fault segment is approximately 6 km long and is located between the Ortakçı segment to the west and the

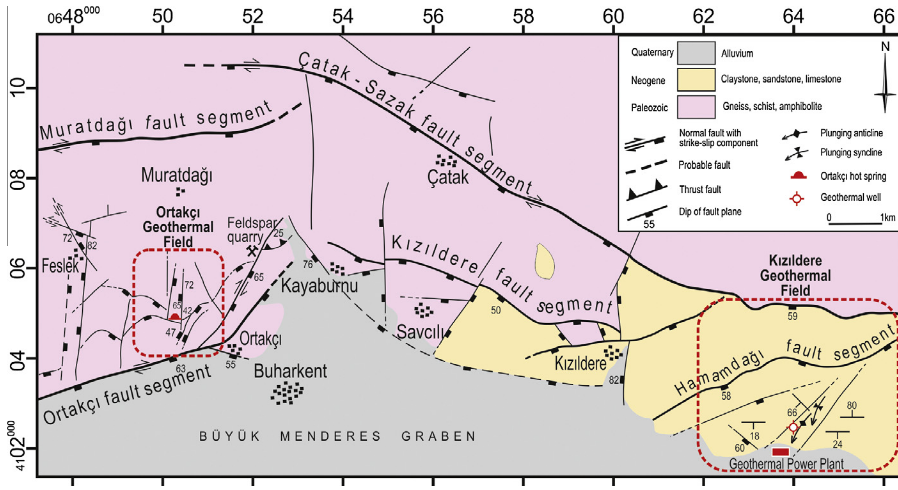

Fig. 6. A geologic and structural map of the Ortakçı and Kızıldere geothermal areas showing the major faults and related minor faults.

Çatak-Sazak fault segment to the east, and it passes through the Kızıldere geothermal field in the E-SE direction. The Kızıldere field has presently the largest installed geothermal capacity (95 MWel) in Turkey, indicating the vast potential on geothermal energy in this region. The scarp morphological signature for this fault suggests a throw at approximately 300 m. The estimated total throw of 600 m for the Çatak-Sazak and Kızıldere faults are compatible with drilling results in the geothermal field.

In the study area, the orientations of the faults in the north of the Büyük Menderes graben are E–W, NE–SW, NW–SE and N–S trending (Figs. 2 and 6). The N–S trending faults developed perpendicular to the approximately E–W trending main fault system, and they are clearly observed in the field as linear valley formations. The Ortakçı hot spring is located at the intersection of the E–W and N–S directed faults (Fig. 3). The E–W directed fault, which is situated immediately north of the Ortakçı fault segment, is southward-dipping and has a length of approximately 4 km. The N–S fault has a left-lateral strike-slip component in the spring area (Fig. 3).

Transverse faults in the study area commonly intersect the main faults at high angles (Figs. 3 and 6). One of the best examples of a NE–SW trending fault in the study area is a transverse fault (cross-fault) of approximately 3 km passing through the village of Ortakçı. The fault terminates at its intersection with the E–W trending Ortakçı fault segment in the south. The fault passes through a feldspar quarry located approximately 2 km north of Ortakçı village (Fig. 3), and it ends near the western tip of the Kızıldere fault segment (Fig. 6). The transverse fault, exhibits a right-lateral strike-slip movement, as demonstrated by the rake of slickensides (140°) on the fault plane located northwest of the Kızıldere fault segment (Fig. 7).

The Ortakçı thermal springs are situated in a relay ramp (also known as an overlap or step-over zone) between overlapping fault segments. The evolution of relay ramps occurs in four different stages, as determined by Peacock and Sanderson (1991, 1994). Based on this definition, the Ortakçı relay ramp is in the 3rd stage, which is characterised by the beginning of fracturing inside the ramp.

The Ortakçı relay ramp is a left-stepping synthetic accommodation zone (Faulds and Varga, 1998) that occurs between similarly dipping (southward) normal or normal oblique-slip fault systems (Figs. 6 and 8a). In the synthetic zone, the relay ramp connects the hanging wall of one fault to that of the next (Peacock and Sanderson, 1991). The width (separation) of the relay ramp between the two normal oblique-slip fault segments is 5 km, whereas the overlap length is approximately 1.6 km

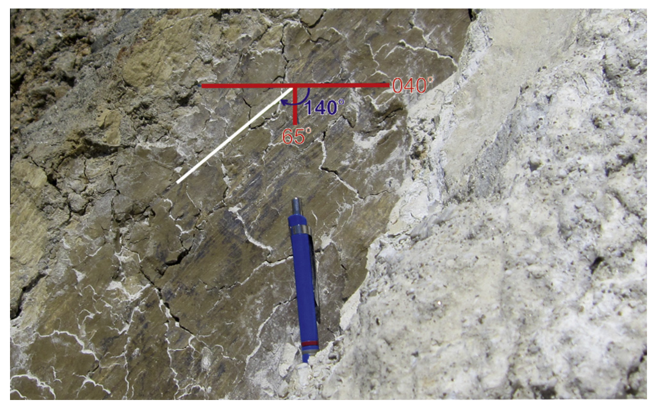

Fig. 7. The fault plane developed between gneiss and amphibolites, including oblique slickensides (rake is 140°), at approximately northeast-southwest-striking and right-lateral fault.

(Figs. 6 and 8a). According to Soliva and Benedicto (2004), the relay ramp in the study area is classified as an "open relay ramp." This classification is based on linkage criterion values (c, overlap/separation ratio), and for the Ortakçı relay ramp, the c values were calculated as 0.32. The Ortakçı relay ramp has a series of small faults at various angles to the main fault plane, creating a varied topography rather than a smooth flexure (Gawthorpe and Hurst, 1993).

The main faults in the area not only display the dip slip component of normal faults, but also a minor right-lateral component. These movements lead to transpressional stresses in the relay ramp between the main fault tips. Therefore, the relay ramp developed as a restraining step-over zone (Fig. 8b and c). The majority of the springs in the graben are located at the intersection of the E–W and N–S or NE–SW striking faults.

Twenty-four fault-slip data have been collected from Ortakçı and Kızıldere thermal spring areas and analysed using TectonicsFP software to understand the kinematic characteristics. To draw the stress diagrams, the slip data of the faults only at the north basin between Pamukören and the east of Kızıldere geothermal power plant were taken into account. Angelier's method (Angelier, 1994) was used for computational processing of the data (Fig. 9a–d). The average attitudes for the estimated stress field orientations are follow $\sigma_1 = 336/73$, $\sigma_2 = 101/12$, $\sigma_3 = 192/22$ (Fig. 9a and b). According to the data obtained from a Numerical Dynamic Analysis (NDA) method, the stress ratio ($R = \sigma_2 - \sigma_3/\sigma_1 - \sigma_3$) was defined as 0.458, which indicates that

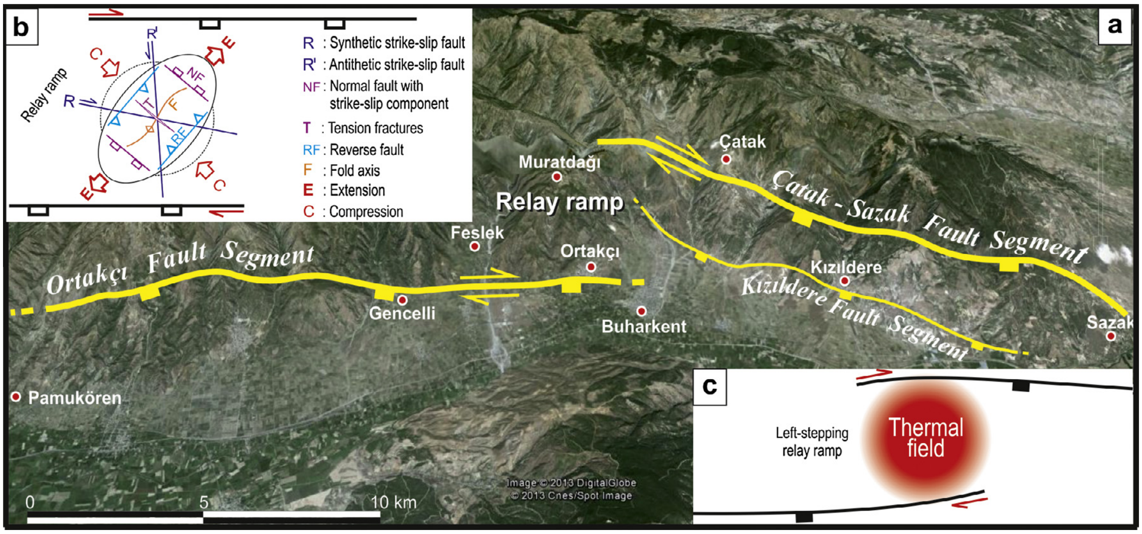

Fig. 8. (a) A satellite image of the step-over zone (relay ramp) between the Ortakçı and Çatak-Sazak fault segments (modified from Google maps, 2013), (b) the structures associated with WNW–ESE directed transpression from the Ortakçı restraining step-over field and (c) a schematic diagram illustrating the plan-view structural sketch of the Ortakçı geothermal area.

the stress regime tension direction (Fig. 9c). The fault slip data show that the neotectonic period is characterised by a subvertical σ_1 and subhorizontal σ_2 and σ_3, that indicate a NNE–SSW tension associated with a deformational system between the Ortakçı, Çatak-Sazak and Muratdağı faults (Figs. 6 and 9).

Three main structural elements were determined in addition to these major faults in the relay ramp: (1) relatively steep (70°) left-lateral strike-slip faults with 70° may reflect N–S Anthithetic Riedel Shear ($\acute{R}$) character and, (2) NE–SW reverse faults with a left-lateral strike-slip component dipping 40–45° to the NW were developed within the contractional relay ramp zone (Figs. 3, 6 and 8). These structures were related to the WNW–ESE direction transpressional stress only within the relay ramp and are compatible with the Riedel deformation model (Wilcox et al., 1973). The σ_1 principal stress is perpendicular to the reverse faults and corresponds to a bisector of acute angle of R′- and R-Riedel strike-slip faults (Fig. 8b). (3) Secondary normal faults with a WNW–ESE direction were developed parallel to transpression direction.

All structural data were obtained from Paleozoic units in the Ortakçı field; therefore, timing of deformation could not be constrained because of the lack of young geologic units. In this context, Neogene clastic rocks were also studied in the Kızıldere Geothermal Field, which is located 10 km east of the Ortakçı field (Fig. 6), to determine clues about young tectonic events. The youngest unit in the Kızıldere field is represented by Late Pliocene aged claystones with conglomerate and sandstone intercalations. In a geothermally operating (KD-15 geothermal well) field, this unit is tightly folded by two faults (with likely oblique normal faults with a major right-lateral strike-slip component. It is because NE-trending faults with similar characteristics have been observed at the adjacent fields), folding may be coeval with faulting; for this reason, a strongly crushed and brecciated hydrothermally altered zone a few kilometres in length was developed along a NE–SW direction. Hinge lines of SE-verging asymmetric folds with vergence direction towards the SE plunge towards the SW. Fold-related bedding attitudes change from 10° to 80° on the narrow field (~1 km^2, Fig. 6). According to the investigation and results, the area has possibly been affected by an approximately WNW–ESE transpression since at least the Pliocene–Pleistocene, based on the age of the youngest unit affected by the folding in the area.

3. Hydrogeological characteristics

The temperature and discharge rate of the Ortakçı hot spring is 50.5 °C and 2.4 l/s, respectively (Gökgöz et al., 2006). The spring consists of meteoric water (almost no tritium content) heated by young tectonic activity and mantle plumes, which are intrude into the upper crustal levels. Süer et al. (2010) pointed out that the $^3He/^4He$ ratios of Tekkehamam waters than the Kızıldere waters are relatively higher and it may indicate that a higher mantle-helium contribution. Similarly, Mutlu et al. (2008) have demonstrated the range ^3He/enthalpy ratios of fluids in western Turkey are consistent with the release of both helium and heat from contemporary supplementations of mantle-derived magmas to the crust. Wiersberg et al. (2011) showed that within the Kızıldere geothermal field, reservoir temperatures and $CO_2/^3He$ and CH_4/C_2H_6 ratios increase and $^3He/^4He$ ratios decrease from southwest to northeast, indicates mixing with cold meteoric water in the reservoir. The hot springs contain no tritium, indicating that the thermal fluids in this field are more than 50 years old (Gökgöz et al., 2006; Şimşek, 2003; Şimşek et al., 2005). Isotopic (^{18}O–D) surveys have detected deep circulation and water–rock interactions in these thermal waters (Şimşek, 2003; Şimşek et al., 2005). Stable isotope values (^{18}O–D) of the geothermal waters indicate a meteoric origin (Mutlu et al., 2008; Süer et al., 2010; Şimşek, 2003). The thermal spring is a $Na–SO_4–HCO_3$ type, and its subsurface temperature, as calculated using chemical geothermometers, is approximately 80 °C at depth 2200 m (Kaya and Gökgöz, 2003).

Hydrothermal alterations associated with fractures in the damaged rocks are also common around the hot spring. These hydrothermal alterations that formed by interaction with the circulating thermal waters are outstanding areas characterised by phyllic, argillic, silicic, hematitised and carbonatised alteration zones (e.g. Özgür, 2002; Karamanderesi and Helvacı, 2003). The influence of extreme crushed and alteration can be detected in the N–S oriented Feslek creek, close to the western portion of the study area. Brown iron oxide coatings are observed on the plane of the N–S trending fault. This mineralization suggests that fluid circulation has occurred during the latest faulting stage, from the Upper Miocene to recent (e.g. Karamanderesi and Helvacı, 2003; Brogi, 2008).

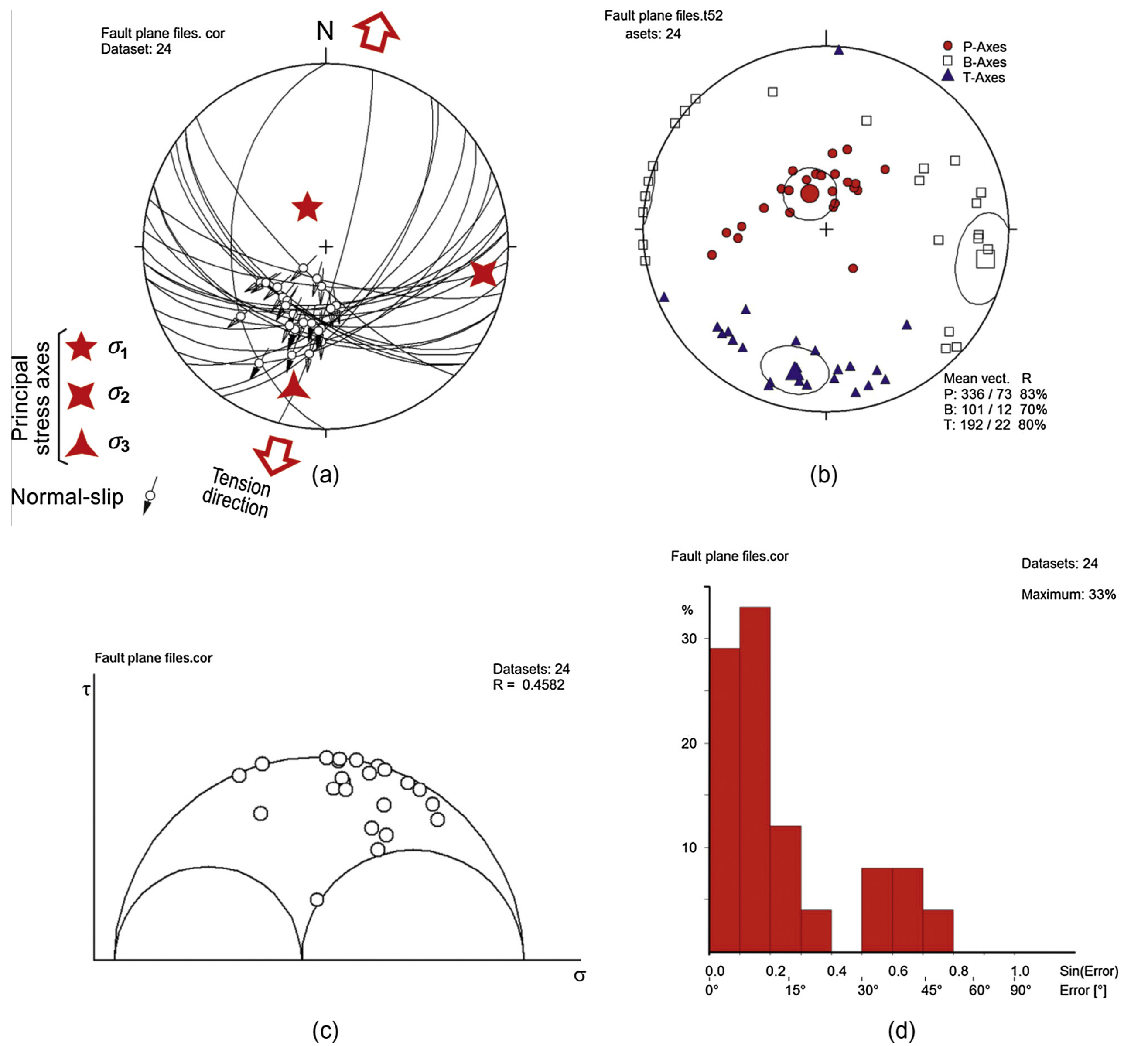

Fig. 9. (a) A Schmidt lower-hemisphere (equal area) projection, Angelier plot of the faults and fault striations were measured in the study area, (b) a PTB-plot of calculated strain axes from kinematic indicators measured on faults slip data, (c) the tectonic regime and stress ratio, expressed by the Mohr–Coulomb stress circle (d) Fluctuation histogram; misfit angle between calculated and measured shear stress vector.

Neogene units are not exposed in this area. The northern margin faults of the graben form a boundary between the Precambrian-Paleozoic Menderes metamorphic series and the Quaternary units (colluviums and alluviums). The Neogene units, however, outcrop 3 km east of Ortakçı village, and probably occur below the Quaternary units in this area.

The Neogene units in the study area are covered by younger units, and no field or borehole data exist for these rocks. Therefore, the data for the Kızıldere geothermal field are based on estimations of the geothermal reservoir features of the Ortakçı field, as these two adjacent fields exhibit very similar lithologic and tectonic features. Furthermore, the Kızıldere field has been well-studied geologically using borehole data (e.g. Karamanderesi, 2013).

The Kızıldere geothermal field has three primary reservoirs: (1) the First (upper) Reservoir, within the Neogene limestones at a depth of 310–375 m, with temperatures of 130–198 °C; (2) the Second Reservoir, within the marble-schist intercalations at a depth of 445–1105 m, with temperatures of 200–212 °C; and (3) the Third (deep) Reservoir, within the gneisses and quartzites that are intercalated with and underlie the schists, with high temperature of 242 °C at a depth of 2261 m (Şimşek, 2003). The geothermal gradient values in the Kızıldere field were determined as 1 to 10 °C/10 m for depths varying between 80 and 250 m in the region (Şimşek, 1985).

4. Discussions

4.1. Structural controls

Three phases of folding have been recognised in the metamorphic rocks, as mentioned in the section on paleotectonic structures. Mesoscopic planar and linear elements and trace of foliation surfaces have been associated with the F_1, F_2 and F_3 folding phases. The neotectonic E–W and N–S directed faults exhibit similar orientations as the paleotectonic E–W second-generation fold (F_2) and N–S third-generation fold (F_3) axial planes. These data indicate that the previously existing fractures parallel to the F_2 and F_3 fold axes have been reactivated during the neotectonic period.

Higher fracture densities and active tectonism are caused by enhanced stress and strain at fault tips (e.g. McGrath and Davison, 1995) and relay ramp zones (Peacock and Sanderson, 1991). Hot springs are usually found in particular structural settings extensively associated with faults; they are most common in relay ramps and are found less commonly at fault-tips and fault intersection points (e.g., Faulds et al., 2010; Curewitz and Karson, 1997). The authors noted that the dynamic continuous (based on the continuation of the fault interactions) hot springs exhibit considerably higher temperatures than kinematic continuous (related to reopening of existing fractures in a breakdown region) hot springs. The circulation of fluids through the crust could be influenced by interconnections between existing discontinuities, including bedding, joints, faults, foliation and igneous contacts (Sibson, 1996). The local stress state, which affects the aperture of existing discontinuities, may show considerable variation in areas of structural overprinting.

The vast majority of the geothermal activity in Turkey is observed in the tectonically active areas of western Turkey, especially in the Büyük Menderes graben. The main fault segments that form the northern and southern boundaries of the relay ramp, branch into multiple splays or horsetail before they terminate (Figs. 3 and 6), generating a belt of higher fracture density and permeability that accommodates significant fluid flow at the fault tips in the Ortakçı region.

Hetzel et al. (2013) demonstrated that during phases of extensional deformation the hydraulic properties of high-angle normal faults and low-angle detachments permitted pervasive meteoric fluid flow along the detachment faults. They document that meteoric fluids infiltrated the upper crustal normal faults and penetrated into the detachments and the upper most levels of their mylonitic footwalls based on Hydrogen isotope (δD) values for fault gouges, cataclasites and mylonites. Also, they exhibit that brittle normal faults are active over ~20 Ma of the extensional history and they are provided effective pathways for meteoric fluids.

The detailed structural features and hydrogeological characteristics of a geothermal field must be investigated to understand the relationships between its cover rocks, reservoir and the circulation of its geothermal fluids (Rotevatn et al., 2007; Brogi, 2008; Giordano et al., 2013). To determine the geothermal play type, all the faults along the active margins of the grabens were mapped (Fig. 10 and Table 1). These data prove that all hot water outflows are related to the high-angle normal faults on hanging wall of the detachment faults. The geothermal fields on the grabens are located on following sites: (a) relay ramps of the normal faults, (b) intersection points of E–W normal and N–S cross faults, (c) multiple splays of terminations of the major faults, (d) parallel/sub-parallel extensional cracks to range front major faults.

The folded beds and fractured zones were influenced by complex stresses (e.g. bending, torsion, tension and shearing) of the relay ramp (Peacock and Sanderson, 1994). Discontinuities such as faults, fractures, fissures, shear zone, bedding and foliation planes in the relay ramp could have allowed leak zones or provided a barrier to fluid flow from the hanging wall to the footwall (e.g. Soliva and Benedicto, 2004). These discontinuities also provide a better flow path for fluids (e.g. Rotevatn et al., 2007).

The main structural factors controlling the movement of thermal fluids are the planes of bedding, faults, fractures, fissures and shear zones associated with the faults. The most important structural elements in the Kızıldere geothermal field are E–W-striking the Çatak-Sazak fault and E–W-striking the high-angle normal faults; N–S and NE–SW-striking faults. The damage zones developed along the faults, presently increasing dilations related to E–W normal faults and the thermal springs located at intersection points constitute the most important pathways for the fluid flow and heat transport. Permeable lithologies containing fractured, bedded, foliated and highly crushed zones in the geothermal field (limestones of the Sazak formation and lithologies consist of the marbles, schists and quartzites of the Menderes massif at the deeper) form the reservoir rock. In addition, they play a very important role for laterally transportion of fluids and heat. These structures were formed not only in the neotectonic period associated with the beginning of graben formation, but also in the palaeotectonic period, during which compressional tectonics created brittle and

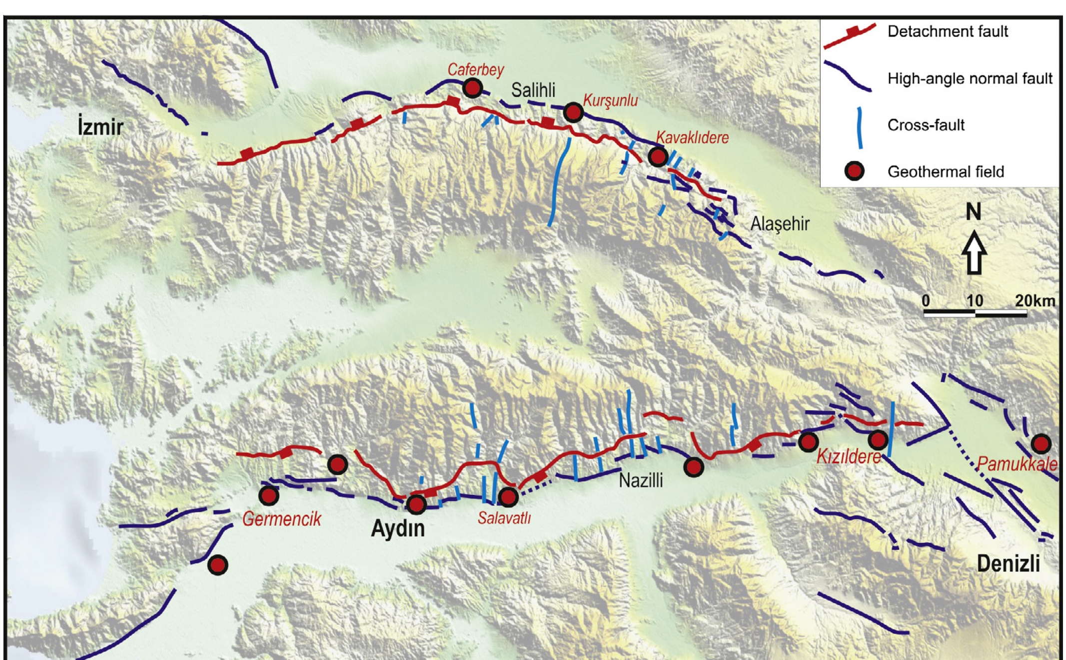

Fig. 10. Structural positions of the geothermal areas developed in front of Büyük Menderes and Gediz detachment faults.

Table 1
Catalog of the geothermal play type of hot springs and geothermal fields associated with the metamorphic core complex formation in Büyük Menderes and Gediz Grabens at the tectonically active margins. BMDF: Büyük Menderes Detachment Fault, GDF: Gediz Detachment Fault, BMG:Büyük Menderes Graben, NF: Normal Fault, SF: Strike-slip Fault, RF: Reverse Fault, TF:Transfer Fault, CF: Cross-fault, HW: Hanging Wall, FC: Fault Controlled, FRC: Fracture controlled, HC: Hydrothermal Circulation.

Geothermal fields/hot springs	Structural setting	Structural characteristics and positions	Heat transport mechanism
Kızıldere	HW of the BMDF with highly S-dipping	Eastern termination of major NF and intersection of the N–S striking CF with E–W striking NF	FC/FRC, HC
Ortakçı	Relay ramp where the BMG bent eastward	Intersection of the E–W striking NF and N–S striking SF	FC, HC
Pamukören Gedik	HW of the BMDF	Intersection of the BMDF and N–S striking CF	FC, HC
Güzelköy Güvendik	HW of the BMDF	Intersection of the BMDF and N–S striking TF	FC
Sultanhisar			
Salavatlı	HW of the BMDF	Intersection of the N–S striking CF and E–W striking RF	FC/FRC, HC
Serçeköy İmamköy Yılmazköy	HW of the BMDF	Intersection of the N–S trending CF with E–W striking NF	FC/FRC, HC
Germencik	HW of the BMDF, BMG where the sharp bent southwestward	Intersection of the N–S trending CF with E–W striking NF, at the western termination of major NF	FC/FRC, HC
Gümüş	HW of the BMDF	Relay ramp of E–W striking NF (Kuşadası fault)	FC, HC
Sazlıköy Tuzburgaz	HW of the BMDF	Relay ramp of NE–SW striking two NF	FC, HC
Horzumsazdere	Gently N-dipping on the HW of the GDF	Intersection of the GDF and N–S striking CF	FC, HC
Kavaklıdere	HW of the GDF	Intersection of the GDF and N–S striking CF	FC, HC
Göbekli	HW of the GDF	Intersection of the GDF and N–S striking CF	FC, HC
Kurşunlu	HW of the GDF	Intersection of the GDF and NW–SE striking dextral SF	FC, HC
Caferbey	HW of the GDF	Intersection of the GDF and NE–SW striking CF	FC, HC

ductile deformation structures. These discontinuous structures allow for the upwelling and circulation of hydrothermal fluids (Sibson, 1996; Hancock et al., 1999; Cox et al., 2001; Brogi, 2004). The fracture-controlled fluid pathways provide fluid flow to the highly permeable fault damage zones deeper than the closely spaced joints, as well as to the bedding near the surface (e.g. Billi et al., 2007; Barbier, 2002).

The fault damage zone, a deformed rock mass surrounding the fault core, includes a well-developed fracture set and a number of small faults and fragmented rock that are more widespread in the hanging wall blocks than in the footwall blocks (Agosta et al., 2006; Brogi, 2008). This zone consists of clusters of deformation bands and discontinuous slip-surfaces that locally supply minor amounts of throw (Shipton and Cowie, 2003). The ENE–WSW trending Ortakçı fault segment has 600 m of vertical throw, whereas the E–W trending Çatak-Sazak and Kızıldere fault segments have 300 m each, for a total 600 m. the width of the damage zone is linearly proportional with fault size, but the maximum deformation density within the damage zone is independent of throw (e.g. Shipton and Cowie, 2003). Regardless of the absolute fault throw and rock type, faults with a large throw up to 600 m have 60–100 m damage zone in the footwall and it is larger in the hanging wall of normal faults and a fault core may develop up to 1 m (Friedman and Wiltschko, 1992; Agosta et al., 2006; Savage and Brodsky, 2011; Johri et al., 2014)

Fractures and deformation bands in damage zones present both problems and opportunities for the circulation of geothermal fluids, depends on the porosity, grain size and lithology permeability increase and decrease (Hancock et al., 1999; Brogi et al., 2003; Fossen et al., 2007, 2011; Schultz et al., 2010; Rotevatn et al., 2013; Johri et al., 2014). The fault cores in the study area are characterised by crushed fault breccias up to 40–50 cm in thickness, representing C-type shear band cleavage as described by Passchier and Trouw (1996) and Brogi (2008).

In the study area, the N–S or NE–SW trending transverse faults that developed orthogonal to or across the E–W trending main fault systems exert significant control over the water flow paths. Hydrothermal fluids prefer to flow into intense damage zones, which are present at the intersections between N–S striking faults and E–W trending main fault segments. The N–S and NE–SW striking faults were steeply dipping, and their provided deep-reaching permeable conduits for fluid upwelling. Therefore, these intersections are important places for the exploration of potential geothermal fields (Faulds et al., 2010).

This thermal field could also be considered a restraining step-over zone between two fault segments whose normal faults have a right-lateral strike component. The faults and fractures passing through the step-over zone suggest that the overlapping faults are connected at depth (Peacock and Parfitt, 2002). Fig. 11a is a schematic sketch illustrating the possible pathway of meteoric waters. This structure indicates that the meteoric waters are joined by intersections in deeper parts of the fault systems and flow through the damage zones of the main faults. Subsequently, the hot water outflows along different pathways occur in relation to the branching of the faults towards the surface.

The structural characteristics of the Ortakçı thermal field step-over zone are comparable to those of the Karahayıt thermal springs field, which is located 30 km east of the study area in a releasing step-over zone of the Pamukkale Fault Zone (e.g. Çakır, 1999; Hancock et al., 1999). The tectonic setting of the study area is also comparable to that of the Pamukören, Güzelköy, Sultanhisar, Salavatlı, Yılmazköy and Germencik geothermal fields (Fig. 1). Similar study approaches have been used in the Larderello (the inner Northern Apennines, southern Tuscany), the Nordfjord-Sogn detachment zone (the Devonian basins in western Norway) and the Basin and Range geothermal fields (the southwestern USA), in which the heat flux and circulation of fluids were associated with shear zones in these tectonically active extensional regions (Brogi et al., 2003; Bellani et al., 2004; Faulds et al., 2009).

4.2. Origin of heat source

Moeck and Beardsmore (2014) have defined a 'geothermal play type' as a model of geothermal system consisting of the combination of structural position and geologic setting. They have suggested which play type might be defined by the heat source and the geological controls on heat transport and thermal energy storage capacity.

4.2.1. Magmatic activity

The Aegean region contains widespread Neogene volcanic rocks, some of which are related to subduction (Fytikas et al., 1984). Volcanic activity has been common in western Turkey since the Late Eocene and is associated with the Eocene continent-arc collision, which continued into Holocene (Aldanmaz et al., 2000). Early Miocene aged granodioritic rocks (Salihli and Turgutlu granodiorite) have been found 50 km north of the study area (Bozdağ region) and to the north of the Ödemiş-Kiraz submassif (Hetzel et al., 1995). Güleç (1991) suggested that The Early-Middle Miocene magmas were generated from a shallow mantle, while the Late Miocene-Quaternary magmas were generated by upwelling deeper mantle source during lithospheric thinning, according to Sr–Nd isotope ratios in volcanic rocks in western Turkey. Furthermore, the Quaternary Kula volcanics, located approximately 60 km north of the study area. The Kula basalts are an example of the rapid uplifting of asthenospheric material in western Anatolia related to an N–S extension (Tokçaer et al., 2005). In this context, the youngest volcanic activity in the region, represented by Kula volcanics, should not to be a heat source origin because of the long distance and lack of recent magmatic activity. Similarly, Faulds et al. (2009) noted that the lack of significant actual magmatic activity indicates that the upper levels of the crust are not a direct heat source for geothermal activity in western Turkey. These authors suggest that most of the geothermal activity in the region is of amagmatic origin. Therefore, the heat source seems to be associated with crustal faulting and is available in different tectonic environments without magmatic activity. According to this data, geothermal play type of the graben is not related to volcanic and plutonic type.

4.2.2. Tectonic activity

The Aegean region is one of the world's most active tectonic areas. Seismic activity related to the faults in the region has been recorded through both historical (Menderes earthquake: 20 September 1899; Nazilli earthquake: 19 December 1645, Güzelhisar/Aydın earthquake: 22 February 1653) and instrumental earthquake observations (Ambraseys and Finkel, 1987, 1995; Altunel, 1999; Ocakoğlu et al., 2013). The fault slip rates obtained from GPS-derived velocity field data from the study area reveal that the total motion of approximately 25 mm/yr corresponds to 10.9 ± 0.3 mm/yr of the left-lateral strike-slip and 14.5 ± 0.3 mm/yr of the normal slip or extension (Reilinger et al., 2006). These slip rate values correspond to deformation ratios (ε) from $0.45 \times 10^{-9}\ s^{-1}$ (34 nanostrain/yr, for normal slip) to $0.80 \times 10^{-9}\ s^{-1}$ (80 nanostrain/yr, for total motion).

Alaşehir and Büyük Menderes detachments are available along the northern and southern margins of the CMM. Detachment faults or shear zones were developed due to thinned-crust tectonics (Wernicke, 1985) within the ductile–brittle transition zone at the upper levels of the continental crust (Fig. 11a). The normal faults and fractures throughout the hanging wall are connected to the main detachment fault in which distributed high stresses are present (e.g. Peacock and Parfitt, 2002).

The presence of low-angle S-dipping detachment faults in the Büyük Menderes graben was confirmed using conventional deep seismic reflection and gravity data defined by three layers in the study area. The first and second layers occur at a thickness of 6 and 13–18 km, and the last one is located at ~33 km, emphasizing the Moho depth (Fig. 11b; Çifçi et al., 2011). Çifçi et al. (2011) reported that seismic reflections were detected up to 16 km in depth, distinguishing the transition zone from the rigid upper crust and the ductile lower crust. Similar data were obtained by Bayrak et al. (2011) for the Kızıldere geothermal field; two deep conductive regions with very low resistivity (< 3 Ω m), which reflects the shallow asthenosphere from two-dimensional resistivity images occurred at depths of ~15 km and ~35 km under the Büyük Menderes graben. Similar values for the continental Moho depth in the region also was obtained by Altınoğlu et al. (2015) using the Bouguer gravity data.

The focal depths of earthquakes in the Büyük Menderes graben were distributed at depths of 5 to 13 km and were concentrated at depths of 5 to 6 km, as determined by compiled data from the USGS (http://www.usgs.gov), AFAD (http://www.deprem.gov.tr) and KOERI (http://www.koeri.boun.edu.tr). These data may be correspond to lithostatic pressure of ~130 MPa and to shear stress of ~110 MPa on the basis of depth (5 km) and dipping (25°) of a major detachment fault plane. The calculated shear stress and deformation rate values are consistent with the values of Molnar and England (1990), which may indicate the required high strain-rates and shear stresses (10^{-11}–$10^{-12}\ s^{-1}$ and ~100 MPa)

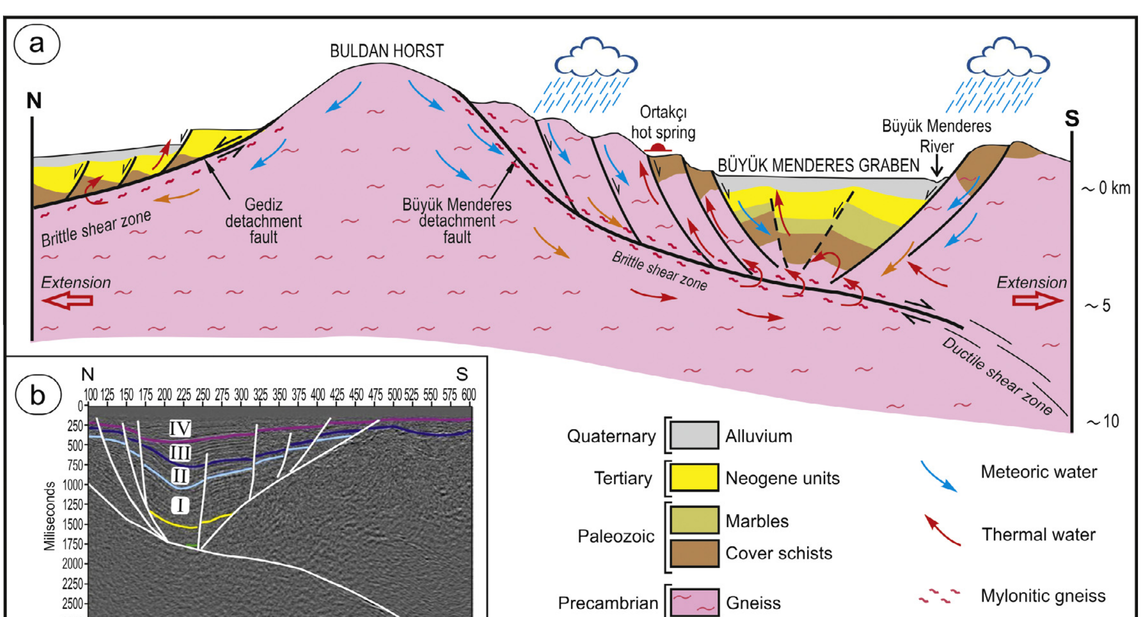

Fig. 11. (a) A conceptual model of geothermal circulation in the study area, (b) a deep seismic profile with the N–S direction taken from a 30 km west of study area (Nazilli region) (Çifçi et al., 2011). Roman numerals indicate the different sedimentary sequences.

for heat production in a shear zone, for a possible heat increase added to the existing high heat flow.

A mean value of heat flow for the western part of Anatolia is approximately 107 ± 45 mV m^{-2}, which is about 60% higher than the world average (İlkışık, 1995). The high heat flow values (140 mV m^{-2}) have been observed at the margins of the northern Büyük Menderes and the southern Gediz grabens (Tezcan, 1995; Fig. 12). The high heat flow corresponds to the places where tectonically active current. The highest heat flow values in the region, compared with other active normal faults are remarkably perfect harmony with detachment faults. This situation indicates that detachment faults are highly effective for the circulating of fluids flow and heat transport (Fig. 11a).

Strain-related heating resulted from the conversion of mechanical energy into heat during progressive deformation in narrow zones (e.g. Brun and Cobbold, 1980). Therefore, heating is an important crustal phenomenon that could be integrated into large-scale tectonic models.

Several hypotheses for the heating of geothermal fluids through tectonic activity are summarised below.

Heat is generated by the friction between two blocks during earthquakes (Kanamori and Heaton, 2000) and is also slowly produced in association with friction events along the brittle-ductile shear zones in the upper levels of the continental crust (e.g. Scholz, 1980; Camacho et al., 2001; Morton et al., 2012; Ben-Zion and Sammis, 2013). The amount of shear heating is mainly dependent on the exhumation rate and the rheological parameters of the rocks (Souche et al., 2013). The localized temperatures of the shear zones at shallow crustal levels are ~200 °C, which are higher than those of surrounding rocks in the Musgrove Block, central Australia (Camacho et al., 2001). In contrast to these proposals, d'Alessio et al. (2003) suggested that the frictional heat increases close to the fault core are not observed in highly localized parts of large faults.

The historical and instrumental earthquake data, in addition to morphologic and geologic data, implies activity on the northern side of the graben with high stresses and deformation rates on the fault planes. These high-dipping faults are connected to a low-angle (θ = 20–25°) major detachment fault at shallow depths (6–13 km, Çifçi et al., 2011) (Fig. 11a and b). The low-angle detachment fault causes higher shear stress and deformation rates where friction/shear generates possible heat sources for thermal areas along the Büyük Menderes graben.

The highest reservoir temperatures of the thermal fields along the Büyük Menderes graben are determined in Kızıldere (242 °C) and Germencik (232 °C) (Fig. 1). The graben bends in these two fields and causes relatively high stress. It has initiated an increase in both dynamically continuous fracture systems and in the temperature. Similarly, there are many hot springs and geothermal resources along the Gediz detachment fault that is in the northern part of the Central Menderes massif (CMM, Fig. 3). The reservoir temperatures along this line are also high, such as at Salihli-Kurşunlu (168 °C), Salihli-Göbekli (182 °C) and Alaşehir-Kavaklıdere (213 °C). These data demonstrate that geothermal resources with high enthalpy are aligned on the northern and southern edges of the CMM, both of which are detachment fault borders (Fig. 10). It gives rise to the argument that the heating source is related to active tectonism, rather than to a magmatic origin.

These data indicate that the mantle is elevated due to N–S crustal extension and thinned controlled by current tectonic activity in western Turkey, heat source of the geothermal fields in the Büyük Menderes and Gediz grabens. Such characteristics reflecting a geothermal system correspond to geothermal play type "extensional domain geothermal play". The elevated mantle provides the principal source of heat for geothermal systems associated with this play type. The resulting high thermal gradients facilitate the heating of meteoric water circulating through deep faults or permeable formations (Moeck and Beardsmore, 2014; Moeck, 2014). The detachment and high-angle normal faults in the area appear to facilitate the deep circulation of the fluids and the transport of heat to surface important pathways (e.g. Brogi et al., 2003; Mutlu et al., 2008; Moeck and Beardsmore, 2014).

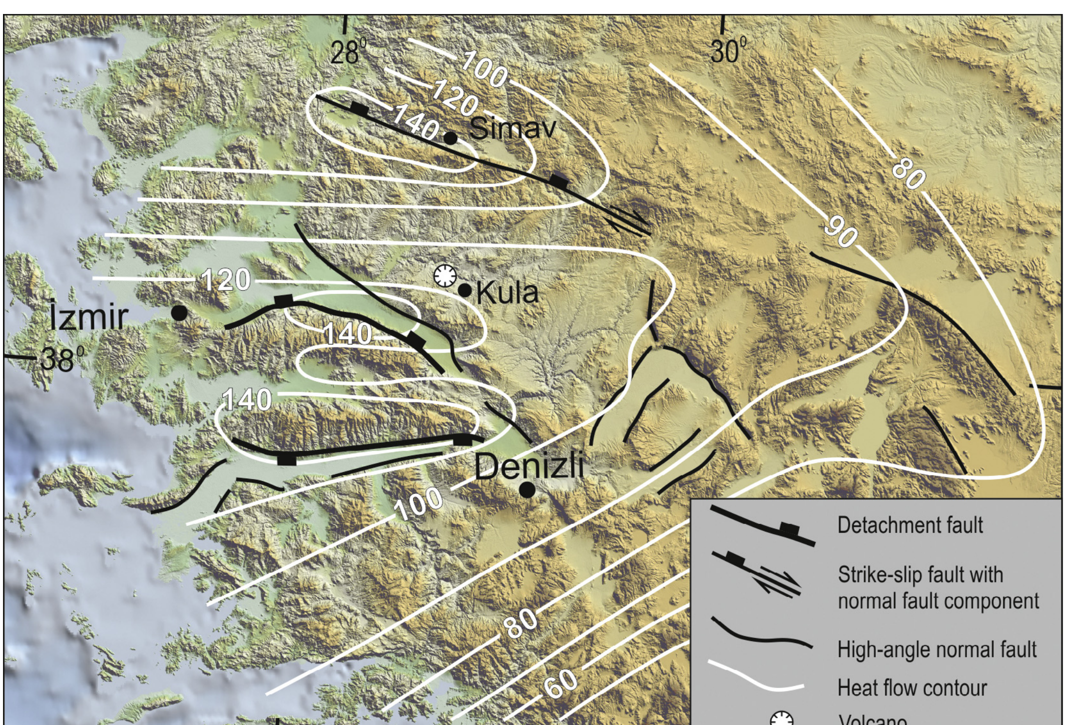

Fig. 12. Heat-flow distribution map (modified from Tezcan, 1995) combined with active tectonic lines of the western Turkey (contour value, mVm-2).

The presence of geothermal fields, hot springs and fumaroles along the northern margin of the Büyük Menderes graben, except for the Tekkehamam thermal field (Fig. 1), indicates that the northern margin faults are tectonically active today. This hypothesis is confirmed by the sedimentological, morphotectonic and seismologic data of the region, as previously stated in the earlier sections. However, the Tekkehamam thermal field, which is the only one located on the southern side of the graben, seems to be associated with a N–S directed transverse fault that cuts perpendicular to the E–W trending main graben faults (Fig. 1).

The thermal springs within the Denizli graben, such as the Yenice, Karahayıt and Pamukkale, are also located on the northern side of a graben with high seismic activity. The N–S striking faults along the Kızıldere-Tekkehamam and other thermal fields are thought to play an active role in the outflow of hydrothermal fluids circulation of the fluids and the transport of heat to surface important pathways.

All of the geothermal areas observed in front of the Büyük Menderes and Gediz detachment faults are related to the high-angle normal faults on hanging wall of the detachment faults. Their structural positions showed that the geothermal fields on the grabens were located on following sites: (a) relay ramps of the normal faults, (b) intersection points of E–W normal and N–S cross faults, (c) multiple splays of terminations of the major faults, (d) parallel/sub-parallel extensional cracks to range front major faults.

The highest heat flow values in the region, compared to other active normal faults were remarkably perfect harmony with detachment faults. This state indicates that detachment faults are highly effective for the circulation of fluid flow and heat transport. Geothermal fields have been intensified on the detachment and the high-normal faults that representing extensional settings, and they indicated potential geothermal sites.

5. Conclusions

The E–W oriented Büyük Menderes graben contains a number of geothermal fields along its northern margin, which reflect the tectonically active parts of the region. The tectonic environment of the study area includes intersecting, overlapping and terminating faults. The Ortakçı hot spring field is located at the intersection of the E–W and N–S directed faults.

The stress ratio (0.458) in the study area indicates the extensional stress regime of NNE–SSW direction. The neotectonic period is characterised by a subvertical σ_1 and subhorizontal σ_2 and σ_3, indicating a NNE–SSW extension associated with a deformational system between the Ortakçı, Çatak-Sazak and Muratdağı fault segments. The relay ramp area has been exposed WSW-ENE directed a transpressional stress regime due to complex stresses.

The primary orientations of the major structural elements in the study area were determined as E–W and N–S for paleotectonic fold and neotectonic fault lineaments, respectively. The N–S trending faults were developed perpendicular to the main E–W fault systems, which formed a right-lateral strike-slip component during the neotectonic period. The neotectonic lineaments seem to have followed inherited fractures and run parallel to the F_2 and F_3-fold axes belonging to a paleotectonic regime, forming the present graben structures. The hot water developed within the relay ramp between the two overlapping E–W fault segments related to the N–S extension.

The N–S trending transverse faults that developed orthogonal to or across the E–W trending fault systems significantly impact the water flow paths of the study area. Thermal fluids prefer to flow in highly fractured zones, which occurred at the intersection between these fault segments, along the shear zones of detachment faults and active normal faults. The hydrothermal outflows that occurred on the relay ramp were permitted by the high permeability fluid-flow conduits formed from the high fracture density and dynamically continuous fracture systems. Lastly, the fault-tips and fault intersection points located within the relay ramps of dynamically extensional regions can be useful starting points for the exploration of potential geothermal fields.

The geothermal play type of the region has been demonstrated by "convection-dominated extension domain" based on structural position of the geothermal areas along the northern and southern margins of the Büyük Menderes and Gediz grabens.

The elevated mantle of thinned lithosphere due to N–S crustal extension controlled by current tectonic activity in western Turkey, is the heat source of the geothermal fields in the Büyük Menderes and Gediz grabens. Geothermal system in the graben corresponds to a "extensional domain geothermal play" type rather than volcanic and plutonic type. The detachment and high-angle normal faults in the area appear to facilitate the deep

References

Agosta, F., Prasad, M., Aydin, A., 2006. Physical properties of carbonate fault rocks, Fucino basin, central Italy: implications for fault seal in platform carbonates. Geofluids 7 (1), 19–32. http://dx.doi.org/10.1111/j.1468-8123.2006.00158.x.

Aldanmaz, E., Pearce, J.A., Thirwall, M.F., Mitchell, J.G., 2000. Petrogenetic evolution of Late Cenozoic, post-collision volcanism in western Anatolia, Turkey. J. Volcanol. Geoth. Res. 102, 67–95. http://dx.doi.org/10.1016/S0377-0273(00)00182-7.

Altınoğlu, F.F., Sarı, M., Aydın, A., 2015. Detection of lineaments in Denizli basin of western Anatolia region using Bouguer gravity data. Pure Appl. Geophys. 172, 415–425. http://dx.doi.org/10.1007/s00024-014-0911-y.

Altunel, E., 1999. Geological and geomorphological observations in relation to the 20 September 1899 Menderes earthquake, Western Turkey. J. Geol. Soc. 156, 241–246. http://dx.doi.org/10.1144/gsjgs.156.2.0241.

Ambraseys, N.N., Finkel, C.F., 1987. Seismicity of Turkey and neighboring regions 1899–1915. Ann. Geophys. 5B, 701–726.

Ambraseys, N.N., Finkel, C.F., 1995. The seismicity of Turkey and adjacent areas: a historical review, 1500–1800. Eren Publication (ISBN 9757622389), Istanbul, Turkey, pp. 240.

Angelier, J., 1994. Fault slip analysis and paleostress field reconstruction. In: Hancock, P.L. (Ed.), Continental Deformation. Pergamon Press, Terrytown, New York, pp. 53–100.

Angelier, J., Lybéris, N., Le Pichon, X., Barrier, E., Huchon, P., 1982. The tectonic development of the Hellenic Arc and the Sea of Crete: a synthesis. Tectonophysics 86 (1–3), 159–196. http://dx.doi.org/10.1016/0040-1951(82)90066-X.

Barbier, E., 2002. Geothermal energy technology and current status: an overview. Renew. Sustain. Energy Rev. 6 (1–2), 3–65. http://dx.doi.org/10.1016/S1364-0321(02)00002-3.

Bayrak, M., Serpen, Ü., İlkışık, O.M., 2011. Two-dimensional resistivity imaging in the Kızıldere geothermal field by MT and DC methods. J. Volcanol. Geoth. Res. 204, 1–11. http://dx.doi.org/10.1016/j.jvolgeores.2011.05.005.

Bellani, S., Brogi, A., Lazzarotto, A., Liotta, D., Ranalli, G., 2004. Heat flow, deep temperatures and extensional structures in the Larderello Geothermal Field (Italy): constraints on geothermal fluid flow. J. Volcanol. Geoth. Res. 132, 15–29. http://dx.doi.org/10.1016/S0377-0273(03)00418-9.

Ben-Zion, Y., Sammis, C.G., 2013. Shear heating during distributed fracturing and pulverization of rocks. Geology 41 (2), 139–142. http://dx.doi.org/10.1130/G33665.1.

Billi, A., Valle, A., Brilli, M., Faccenna, C., Funiciello, R., 2007. Fracture-controlled fluid circulation and dissolutional weathering in sinkhole-prone carbonate rocks from central Italy. J. Struct. Geol. 29, 385–395. http://dx.doi.org/10.1016/j.jsg.2006.09.008.

Bozkurt, E., 2000. Timing of extension on the Büyük Menderes Graben, western Turkey, and its tectonic implications. In: Bozkurt, E., Winchester, J.A., Piper, J.D.A. (Eds.), Tectonics and Magmatism in Turkey and the Surrounding Area. Geological Society, London, Special Publication 173, pp. 385–403.

Bozkurt, E., 2003. Origin of NNE-trending basins in Western Turkey. Geodin. Acta 16 (2–6), 61–81. http://dx.doi.org/10.1016/S0985-3111(03)00002-0.

Bozkurt, E., Rojay, B., 2005. Episodic, two-stage Neogene extension and short-term intervening compression in western Turkey: field evidence from the Kiraz Basin and Bozdağ Horst. Geodin. Acta 18 (3–4), 299–316. http://dx.doi.org/10.3166/ga.18.299-316.

Bozkurt, E., Sözbilir, H., 2004. Tectonic evolution of the Gediz Graben: field evidence for an episodic, two-stage extension in western Turkey. Geol. Mag. 141 (1), 63–79. http://dx.doi.org/10.1017/S0016756803008379.

Brogi, A., 2004. Faults linkage, damage rocks and hydrothermal fluid circulation: tectonic interpretation of the Rapolano Terme travertines (southern Tuscany, Italy) in the context of Northern Apennines Neogene-Quaternary extension. Eclogae Geol. Helv. 97 (3), 307–320. http://dx.doi.org/10.1007/s00015-004-1134-5.

Brogi, A., 2008. Faults zone architecture and permeability features in siliceous sedimentary rocks: insights from the Rapolano geothermal area (Northern Apennines, Italy). J. Struct. Geol. 30, 237–256. http://dx.doi.org/10.1016/j.jsg.2007.10.004.

Brogi, A., Lazzarotto, A., Liotta, D., Ranalli, G., 2003. Extensional shear zones as imaged by reflection seismic lines: the Larderello geothermal field (central Italy). Tectonophysics 363 (1–2), 127–139. http://dx.doi.org/10.1016/S0040-1951(02)00668-6.

Brun, J.P., Cobbold, P.R., 1980. Strain heating and thermal softening in continental shear zones: a review. J. Struct. Geol. 2, 149–158. http://dx.doi.org/10.1016/0191-8141(80)90045-0.

Camacho, A., McDougall, I., Armstrong, R., Braun, J., 2001. Evidence for shear heating, Musgrave Block, Central Australia. J. Struct. Geol. 23, 1007–1013. http://dx.doi.org/10.1016/S0191-8141(00)00172-3.

Catlos, E.J., Çemen, İ., 2005. Monazite ages and the evolution of the Menderes Massif, western Turkey. Int. J. Earth Sci. 94 (2), 204–217. http://dx.doi.org/10.1007/s00531-005-0470-7.

Cox, S.F., Braun, J., Knackstedt, M.A., 2001. Principles of structural control on permeability and fluid flow in hydrothermal systems. Rev. Econ. Geol. 14, 1–24.

Curewitz, D., Karson, J.A., 1997. Structural settings of hydrothermal outflow: fracture permeability maintained by fault propagation and interaction. J. Volcanol. Geoth. Res. 79, 149–168. http://dx.doi.org/10.1016/S0377-0273(97)00027-9.

Çakır, Z., 1999. Along-strike discontinuity of active normal faults and its influence on Quaternary travertine deposition; examples from western Turkey. Turkish J. Earth Sci. 14, 67–80.

Çifçi, G., Pamukcu, O., Çoruh, C., Çopur, S., Sözbilir, H., 2011. Shallow and Deep Structure of a Supradetachment Basin Based on Geological, Conventional Deep Seismic Reflection Sections and Gravity Data in the Büyük Menderes Graben, Western Anatolia. Surv. Geophys. 32, 271–290. http://dx.doi.org/10.1007/s10712-010-9109-8.

d'Alessio, M., Blythe, A.E., Bürgmann, R., 2003. No frictional heat along the San Gabriel fault, California: evidence from fission track thermochronology. Geology 31 (6), 541–544. http://dx.doi.org/10.1130/0091-7613(2003) 0312.0.CO;2.

Davis, G.H., 1983. Shear-zone model for the origin of metamorphic core complexes. Geology 11, 342–347. http://dx.doi.org/10.1130/0091-7613(1983)11<342:SMFTOO>2.0.CO;2.

Dewey, J.F., 1988. Extensional collapse of orogens. Tectonics 7, 1123–1139. http://dx.doi.org/10.1029/TC007i006p01123.

Dewey, J.F., Şengör, A.M.C., 1979. Aegean and surrounding region: complex multiplate and continuum tectonics in a convergent zone. Geol. Soc. Am. Bull. 90, 84–92. http://dx.doi.org/10.1130/0016-7606(1979) 90<84:AASRCM>2.0.CO;2.

Dora, O.Ö., 2011. The historical development of geological investigations in the Menderes massif (in Turkish). Bull. Miner. Res. Explor. Inst. Turkey 142, 1–23.

Dora, O.Ö., Kun, N., Candan, O., 1990. Metamorphic history and geotectonic evolution of the Menderes Massif. In: Proceedings of the International Earth Sciences Congress on Aegean Regions, Izmir, vol. 2, pp. 102–115.

Faulds, J.E., Bouchot, V., Moeck, I., Oğuz, K., 2009. Structural controls on geothermal systems in western Turkey: a preliminary report. GRC Transact. 33, 375–381.

Faulds, J.E., Coolbaugh, M., Bouchot, V., Moeck, I., Oguz, K., 2010. Characterizing structural controls of geothermal reservoirs in the basin and range, USA, and western Turkey: developing successful exploration strategies in extended terranes. In: Proceedings of the WGC, April 25–30, Bali, Indonesia, 1163: p. 11.

Faulds, J.E., Varga, R.J., 1998. The role of accommodation zones and transfer zones in the regional segmentation of extended terranes. Geol. Soc. Am. Spec. Pap. 323, 1–45. http://dx.doi.org/10.1130/0-8137-2323-X.1.

Fossen, H., Schultz, R.A., Shipton, Z.K., Mair, K., 2007. Deformation bands in sandstone: a review. J. Geol. Soc., Lond. 164 (06036), 1–15.

Fossen, H., Schultz, R.A., Torabi, A., 2011. Conditions and implications for compaction band formation in the Navajo Sandstone, Utah. J. Struct. Geol. 33 (10), 1477–1490. http://dx.doi.org/10.1016/j.jsg.2011.08.001.

Friedman, N.M., Wiltschko, D.V., 1992. An approach to exploration for naturally fractured reservoirs, with examples from the Austin Chalk. In: Schmoker, J.W, Coalson, E.B., Brown, C.A. (Eds.), Geological Studies Relevant to Horizontal Drilling; Examples from Western North America: Rocky Mountain Association of Geologists (RMAG), Denver, CO., pp. 143–153.

Fytikas, M., Innocenti, F., Manetti, P., Mazuoli, R., Peccerilo, A., Villari, L., 1984. Tertiary to Quaternary evolution of the volcanism in the Aegean region. In: Dixon, J.E., Robertson, A.H.F. (Eds.), The Geological Evolution of the Eastern Mediterranean. Geological Society of London, Special Publications 17, pp. 687–699. http://dx.doi.org/10.1144/GSL.SP.1984.017.01.55.

Gawthorpe, R.L., Hurst, J.M., 1993. Transfer zones in extensional basins: their structural style and influence on drainage development and stratigraphy. J. Geol. Soc. 150, 1137–1152. http://dx.doi.org/10.1144/gsjgs.150.6.1137.

Gessner, K., Gallardo, L.A., Markwitz, V., Ring, U., Thomson, S.N., 2013. What caused the denudation of the Menderes Massif: review of crustal evolution, lithosphere structure, and dynamic topography in southwest Turkey. Gondwana Res. 24 (1), 243–274. http://dx.doi.org/10.1016/j.gr.2013.01.005.

Gessner, K., Ring, U., Johnson, C., Hetzel, R., Passhier, G.W., Güngör, T., 2001. An active bivergent rolling-hinge detachment system: Central Menderes metamorphic core complex in western Turkey. Geology 29 (7), 611–614. http://dx.doi.org/10.1130/0091-7613(2001) 029<0611:AABRHD>2.0.CO;2.

Giordano, G., Pinton, A., Cianfarra, P., Baez, W., Chiodi, A., Viramonte, J., Norini, G., Groppelli, G., 2013. J. Volcanol. Geoth. Res. 249, 77–94.

Gökgöz, A., Kaya, A., Kaya, M., 2006. Geology and hydrochemistry properties of the Ortakçı thermal spring (Aydın). In: 30th Anniversary Fikret Kurtman Geology Symposium. Abstracts, Selçuk University, Konya, pp. 183–184.

Güleç, N., 1991. Crust–mantle interaction in western Turkey: implications from Sr and Nd isotope geochemistry of Tertiary and Quaternary volcanics. Geol. Mag. 128 (05), 417–435. http://dx.doi.org/10.1017/S0016756800018604.

Gürer, Ö.M., Sarıca-Filoreau, N., Özburan, M., Sangu, E., Doğan, B., 2009. Progressive development of the Büyük Menderes Graben based on new data, western Turkey. Geol. Mag. 146 (05), 652–673. http://dx.doi.org/10.1017/S0016756809006359.

Hancock, P.L., Chalmers, R.M.L., Altunel, E., Çakir, Z., 1999. Travitonics: using travertines in active fault studies. J. Struct. Geol. 21, 903–916. http://dx.doi.org/10.1016/S0191-8141(99)00061-9.

Hetzel, R., Passchier, C.W., Ring, U., Dora, O.Ö., 1995. Bivergent extension in orogenic belts: the Menderes Massif (southwestern Turkey). Geology 23, 455–458. http://dx.doi.org/10.1130/0091-7613(1995) 023<0455:BEIOBT>2.3.CO;2.

Hetzel, R., Reischmann, T., 1996. Intrusion Age of Pan-African Augen Gneisses in the Southern Menderes Massif and the Age of Cooling after Alpine Ductile Extensional Deformation. Geol. Mag. 133 (5), 565–572.

Hetzel, R., Romer, R.L., Candan, O., Passchier, C.W., 1998. Geology of the Bozdağ area, central Menderes Massif, SW Turkey: Pan-African basement and Alpine deformation. Geol. Rundsch. 87, 394–406. http://dx.doi.org/10.1007/s005310050218.

Hetzel, R., Zwingmann, H., Mulch, A., Gessner, K., Akal, C., Hampel, A., Güngör, T., Petschick, R., Mikes, T., Wedin, F., 2013. Spatiotemporal evolution of brittle normal faulting and fluid infiltration in detachment fault systems: a case study from the Menderes Massif, western Turkey. Tectonics 32 (3), 364–376. http://dx.doi.org/10.1002/tect.20031.

Işık, V., Seyitoğlu, G., Çemen, İ., 2003. Ductile–brittle transition along the Alasehir detachment fault and its structural relationship with the Simav detachment fault, Menderes massif, western Turkey. Tectonophysics 374, 1–18. http://dx.doi.org/10.1016/S0040-1951(03)00275-0.

İlkışık, O.M., 1995. Regional heat flow in western Anatolia using silica temperature estimates from thermal springs. Tectonophysics 244 (1–3), 175–184. http://dx.doi.org/10.1016/0040-1951(94)00226-Y.

Jackson, J., 1994. Active tectonics of the Aegean region. Annu. Rev. Earth Planet. Sci. 22, 239–271. http://dx.doi.org/10.1146/annurev.ea.22.050194.001323.

Jackson, J.A., McKenzie, D.P., 1988. Rates of active deformation in the Aegean Sea and surrounding regions. Basin Res. 1, 121–128. http://dx.doi.org/10.1111/j.1365-2117.1988.tb00009.x.

Johri, M., Dunham, E.M., Zoback, M.D., Fang, Z., 2014. Predicting fault damage zones by modeling dynamic rupture propagation and comparison with field observations. J. Geophys. Res.: Solid Earth 119 (2), 1251–1272. http://dx.doi.org/10.1002/2013JB010335.

Kanamori, H., Heaton, T.H., 2000. Microscopic and macroscopic physics of Earthquakes. In: Rundle, J.B.D., Turcotte, L., Klein, W. (Eds.), GeoComplexity and the Physics of Earthquakes. American Geophysical Union, Washington, D.C. Geophysical Monograph Series 120, pp. 147–163.

Karakuş, H., Şimşek, Ş., 2013. Tracing deep thermal water circulation systems in the E–W trending Büyük Menderes Graben, western Turkey. J. Volcanol. Geoth. Res. 252, 38–52.

Karamanderesi, İ.H., 2013. Characteristics of Geothemal Reservoirs in Turkey. In: Bracke, R., Harvey, C., Ruter, H. (Eds.), Geothermal Exploration Best Practices. IFC – International Finance Corporation Developers Workshop, 18–19 November, Izmir, Turkey. IGA Academy Report (1), 0102–2013, p. 34.

Karamanderesi, İ.H., Helvacı, C., 2003. Geology and Hydrothermal Alteration of the Aydın-Salavatlı Geothermal Field, Western Anatolia, Turkey. Turkish J. Earth Sci. 12, 175–198. http://dx.doi.org/10.1016/j.jvolgeores.2012.11.006.

Karamanderesi, İ.H., Ölçenoğlu, K., 2005. Geology of the Denizli Sarayköy (Gerali) Geothermal Field, western Anatolia, Turkey. In: Proceedings World Geothermal Congress, 24–29 April 2005, Antalya, Turkey, p. 10.

Kaya, M., Gökgöz, A., 2003. Hydrogeochemical investigation of Ortakçı hot and mineralized spring (Buharkent-Aydın) (in Turkish). Pamukkale Univ. J. Eng. Sci. 11 (2), 257–266.

Kazancı, N., Dündar, S., Alçiçek, M.C., Gürbüz, A., 2009. Quaternary deposits of the Büyük Menderes Graben in western Anatolia, Turkey: implications for river capture and the longest Holocene estuary in the Aegean Sea. Mar. Geol. 264 (3–4), 165–176. http://dx.doi.org/10.1016/j.margeo.2009.05.003.

Kerrich, R., 1986. Fluid infiltration into fault zones: chemical, isotopic and mechanical effects. Pure Appl. Geophys. 124 (1–2), 225–268. http://dx.doi.org/10.1007/BF00875727.

Koçyiğit, A., 2005. The Denizli graben-horst system and the eastern limit of western Anatolian continental extension: basin fill, structure, deformational mode, throw amount and episodic evolutionary history, SW Turkey. Geodinam. Acta 18 (3–4), 167–208. http://dx.doi.org/10.3166/ga.18.167-208.

Koçyiğit, A., Yusufoğlu, H., Bozkurt, E., 1999. Evidence from the Gediz graben for episodic two-stage extension in western Turkey. J. Geol. Soc. Lond. 156, 605–616. http://dx.doi.org/10.1144/gsjgs.156.3.0605.

Koralay, O.E., Candan, O., Chen, F., Akal, C., Oberhänsli, R., Satır, M., Dora, O.Ö., 2012. Pan-African magmatism in the Menderes Massif: geochronological data from leucocratic tourmaline orthogneisses in western Turkey. Int. J. Earth Sci. 101 (8), 2055–2081. http://dx.doi.org/10.1007/s00531-012-0775-2.

Le Pichon, X., Angelier, J., 1981. The Aegean Sea: Philosophical Transactions of the Royal Society of London, Series A, Mathematical and Physical Sciences, vol. 300 (1454), pp. 357–372.

Lips, A.L.W., Cassard, D., Sözbilir, H., Yılmaz, H., 2001. Multistage exhumation of the Menderes Massif, western Anatolia (Turkey). Int. J. Earth Sci. 89, 781–792. http://dx.doi.org/10.1007/s005310000101.

Lister, G.S., Davis, G.A., 1989. The origin of metamorphic core complexes and detachment faults formed during Tertiary continental extension in the northern Colorado River region, USA. J. Struct. Geol. 11 (1–2), 65–69. http://dx.doi.org/10.1016/0191-8141(89)90036-9.

McGrath, A.G., Davison, I., 1995. Damage zone geometry around fault tips. J. Struct. Geol. 17 (7), 1011–1024. http://dx.doi.org/10.1016/0191-8141(94)00116-H.

McKenzie, D., 1978. Active tectonics of the Alpine-Himalayan belt: the Aegean Sea and surrounding regions. Geophys. J. Roy. Astron. Soc. 55 (1), 217–254. http://dx.doi.org/10.1111/j.1365-246X.1978.tb04759.x.

Moeck, I.S., 2014. Catalog of geothermal play types based on geologic controls. Renew. Sustain. Energy Rev. 37, 867–882. http://dx.doi.org/10.1016/j.rser.2014.05.032.

Moeck, I.S., Beardsmore, G., 2014. A New 'Geothermal Play Type' Catalog: Streamlining Exploration Decision Making. In: Proceedings. Thirty-Ninth Workshop on Geothermal Reservoir Engineering; February 24–26, Stanford University, Stanford, California, SGP-TR-202, pp. 8.

Molnar, P., England, P., 1990. Temperatures, heat flux and frictional stress near major thrust faults. J. Geophys. Res. 95 (B4), 4833–4856. http://dx.doi.org/10.1029/JB095iB04p04833.

Morton, N., Girty, G.H., Rockwell, T.K., 2012. Fault zone architecture of the San Jacinto fault zone in Horse Canyon, southern California: a model for focused post-seismic fluid flow and heat transfer in the shallow crust. Earth Planet. Sci. Lett. 329–330, 71–83. http://dx.doi.org/10.1016/j.epsl.2012.02.013.

Mutlu, H., Güleç, N., Hilton, D.R., 2008. Helium-carbon relationships in geothermal fluids of western Anatolia, Turkey. Chem. Geol. 247 (1–2), 305–321. http://dx.doi.org/10.1016/j.chemgeo.2007.10.021.

Norton, D., Knapp, R., 1977. Transport phenomena in hydrothermal systems; the nature of porosity. Am. J. Sci. 277, 913–936.

Ocakoğlu, F., Açıkalın, S., Güneş, G., Özkes, Dirik, K., Özsayın, E., 2013. Was the 1899 Menderes Valley Earthquake a double earthquake? Historical and paleosismological constraints. J. Asian Earth Sci. 67–68, 187–198. http://dx.doi.org/10.1016/j.jseaes.2013.02.026.

Özgür, N., 2002. Geochemical Signature of the Kizildere Geothermal Field, Western Anatolia, Turkey. Int. Geol. Rev. 44, 153–163. http://dx.doi.org/10.2747/0020-6814.44.2.153.

Passchier, C.W., Trouw, R.A.J., 1996. Microtectonics. Springer-Verlag, Berlin, pp. 289.

Peacock, D.C.P., Parfitt, E.A., 2002. Active relay ramps and normal fault propagation on Kilauea Volcano, Hawaii. J. Struct. Geol. 24, 729–742. http://dx.doi.org/10.1016/S0191-8141(01)00109-2.

Peacock, D.C.P., Sanderson, D.J., 1991. Displacements, segment linkage and relay ramps in normal fault zones. J. Struct. Geol. 13 (6), 721–733.

Peacock, D.C.P., Sanderson, D.J., 1994. Geometry and development of relay ramps in normal fault systems. Am. Assoc. Petrol. Geol. Bull. 78 (2), 147–165. http://dx.doi.org/10.1016/0191-8141(91)90033-F.

Purvis, M., Robertson, A.H.F., 2004. A pulsed extension model for the Neogene-Recent E–W-trending Alasehir Graben and the NE–SW-trending Selendi and Gördes Basins, western Turkey. Tectonophysics 391, 171–201. http://dx.doi.org/10.1016/j.tecto.2004.07.011.

Reilinger, R., McClusky, S., Vernant, P., Lawrence, S., Ergintav, S., Cakmak, R., Ozener, H., Kadirov, F., Guliev, I., Stepanyan, R., Nadariya, M., Hahubia, G., Mahmoud, S., Sakr, K., ArRajehi, A., Paradissis, D., Al-Aydrus, A., Prilepin, M., Guseva, T., Evren, E., Dmitrotsa, A., Filikov, S.V., Gomez, G., Al-Ghazzi, R., Karam, G., 2006. GPS constraints on continental deformation in the Africa–Arabia–Eurasia continental collision zone and implications for the dynamics of plate interactions. J. Geophys. Res.-Solid Earth 111 (B5), B05411. http://dx.doi.org/10.1029/2005JB004051.

Rimmele, G., Oberhansli, R., Goffe, B., Jolivet, L., Candan, O., Çetinkaplan, M., 2003. First evidence of high-pressure metamorphism in the "Cover Series" of the southern Menderes Massif. Tectonic and metamorphic implications for the evolution of SW Turkey. Lithos 71 (1), 19–46. http://dx.doi.org/10.1016/S0024-4937(03)00089-6.

Rotevatn, A., Fossen, H., Hesthammer, J., Aas, T.E., Howell, J.A., 2007. Are relay ramps conduits for fluid flow? Structural analysis of relay ramp in Arches National Park, Utah. In: Lonergan, L., Jolly, R.J.H., Rawnsley, K., Sanderson, D.J. (Eds.), Fractured Reservoirs. The Geological Society of London, Special Publications 270, pp. 55–71. http://dx.doi.org/10.1144/GSL.SP.2007.270.01.04.

Rotevatn, A., Sandve, T.H., Keilegavlen, E., Kolyukhin, D., Fossen, H., 2013. Deformation bands and their impact on fluid flow in sandstone reservoirs: the role of natural thickness variations. Geofluids 13 (3), 359–371. http://dx.doi.org/10.1111/gfl.12030.

Savage, H.M., Brodsky, E.E., 2011. Collateral damage: evolution with displacement of fracture distribution and secondary fault strands in fault damage zones. J. Geophys. Res.: Solid Earth 166 (B03405), 14. http://dx.doi.org/10.1029/2010JB007665.

Scholz, C.H., 1980. Shear heating and state of stress on faults. J. Geophys. Res.: Solid Earth 8 (B11), 6174–6184. http://dx.doi.org/10.1029/JB085iB11p06174.

Schultz, R.A., Okubo, C.H., Fossen, H., 2010. Porosity and grain size controls on compaction band formation in Jurassic Navajo Sandstone. Geophys. Res. Lett. 37 (22). http://dx.doi.org/10.1029/2010GL044909, L22306, p.5.

Seyitoğlu, G., Çemen, İ., Şen, Ş., Işık, V., 2002. Extensional tectonics and related basin development in western Turkey. In Extensional Tectonics in the Southern Basins and Ranges, United States, and in Western Turkey. Denver Annual Meeting (October 27–30), Abstracts with Programs, The Geological Society of America, Session no 79.

Seyitoğlu, G., Scott, B.C., 1991. Late Cenozoic crustal extension and basin formation in west Turkey. Geol. Mag. 128, 155–166.

Seyitoğlu, G., Scott, B.C., 1996. The cause of N–S extensional tectonics in western Turkey: tectonic escape vs Back-arc spreading vs Orogenic collapse. J. Geodyn. 22 (1–2), 145–153. http://dx.doi.org/10.1016/0264-3707(96)00004-X.

Seyitoğlu, G., Scott, B.C., Rundle, C.C., 1992. Timing of Cenozoic extensional tectonics in west Turkey. J. Geol. Soc. 149 (4), 533–538. http://dx.doi.org/10.1144/gsjgs.149.4.0533.

Shipton, Z.K., Cowie, P.A., 2003. A conceptual model for the origin of fault damage zone structures in high-porosity sandstone. J. Struct. Geol. 25, 333–344. http://dx.doi.org/10.1016/S0191-8141(02)00037-8.

Sibson, R.H., 1996. Structural permeability of fluid-driven fault-fracture meshes. J. Struct. Geol. 18 (8), 1031–1042. http://dx.doi.org/10.1016/0191-8141(96)00032-6.

Soliva, R., Benedicto, A., 2004. A linkage criterion for segmented normal faults. J. Struct. Geol. 26, 2251–2267. http://dx.doi.org/10.1016/j.jsg.2004.06.008.

Souche, A., Medvedev, S., Andersen, T.B., Dabrowski, M., 2013. Shear heating in extensional detachments: Implications for the thermal history of the Devonian basins of W Norway. Tectonophysics 608, 1073–1085. http://dx.doi.org/10.1016/j.tecto.2013.07.005.

Sözbilir, H., 2005. Oligo-Miocene extension in the Lycian orogen: evidence from the Lycian molasse basin, SW Turkey. Geodinam. Acta 18 (3–4), 255–282. http://dx.doi.org/10.3166/ga.18.255-282.

Süer, S., Wiersberg, T., Güleç, N., Erzinger, J., Parlaktuna, M., 2010. Geochemical Monitoring of the Seismic Activities and Noble Gas Characterization of the Geothermal Fields along the Eastern Segment of the Büyük Menderes Graben. In: Proceedings World Geothermal Congress, 25–29 April, Bali, Indonesia, p. 8.

Şengör, A.M.C., 1982. Factors governing the neotectonic evolution of the Aegean. In: Erol, O., Oygür, V. (Eds.), Young Tectonics and Volcanism of Western Anatolia Panel. Geological Congress of Turkey, Ankara, pp. 59–71 (in Turkish).

Şengör, A.M.C., 1987. Cross-faults and differential stretching of hanging walls in regions of low-angle normal faulting: examples from western Turkey. Geol. Soc., Lond., Spec. Publ. 28, 575–589. http://dx.doi.org/10.1144/GSL.SP.1987.028.01.38.

Şengör, A.M.C., Bozkurt, E., 2013. Layer-parallel shortening and related structures in zones undergoing active regional pure horizontal extension. Int. J. Earth Sci. 102, 101–119.

Şengör, A.M.C., Satır, M., Akkök, R., 1984. Timing of tectonic events in the Menderes Massif, Western Turkey: implications for tectonic evolution and evidence for Pan-African basement in Turkey. Tectonics 3 (7), 693–707. http://dx.doi.org/10.1029/TC003i007p00693.

Şengör, A.M.C., Yılmaz, Y., 1981. Tethyan evolution of Turkey: a plate tectonic approach. Tectonophysics 75, 181–241. http://dx.doi.org/10.1016/0040-1951(81)90275-4.

Şimşek, Ş., 1985. Geothermal model of Denizli, Sarayköy-Buldan area. Geothermic 14 (2–3), 393–417. http://dx.doi.org/10.1016/0375-6505(85)90078-1.

Şimşek, Ş., 2003. Hydrogeological and isotopic survey of geothermal fields in the Büyük Menderes Graben, Turkey. Geothermics 32, 669–678. http://dx.doi.org/10.1016/S0375-6505(03)00072-5.

Şimşek, Ş., Yıldırım, N., Gülgör, A., 2005. Developmental and environmental effects of the Kızıldere geothermal power project, Turkey. Geothermics 34, 239–256. http://dx.doi.org/10.1016/j.geothermics.2004.12.005.

Taymaz, T., Jackson, J.A., McKenzie, D.P., 1991. Active tectonics of the north and central Aegean Sea. Geophys. J. Int. 106 (2), 433–490. http://dx.doi.org/10.1111/j.1365-246X.1991.tb03906.x.

Tezcan, A.K., 1995. Geothermal exploration and heat flow in Turkey. In: Gupta, M.L., Yamano, M., (Eds.), Terrestrial Heat Flow and Geothermal Energy in Asia. Oxford and IBH publishing Co., Pvt. Ltd., New Delhi, pp. 23–42.

Tokçaer, M., Agostini, S., Savaşçın, M.Y., 2005. Geotectonic Setting and Origin of the Youngest Kula Volcanics (Western Anatolia), with a New Emplacement Model. Turkish J. Earth Sci. 14 (2), 145–166.

Van Hinsbergen, D.J.J., Dekkers, M.J., Bozkurt, E., Koopman, M., 2010. Exhumation with a twist: paleomagnetic constraints on the evolution of the Menderes metamorphic core complex (western Turkey). Tectonics 29. http://dx.doi.org/10.1029/2009TC002596, pp. TC3009, 1–33.

Wernicke, B., 1985. Uniform-sense normal simple shear of the continental lithosphere. Can. J. Earth Sci. 22, 108–125. http://dx.doi.org/10.1139/e85-009.

Wiersberg, T., Süer, S., Güleç, N., Erzinger, J., Parlaktuna, M., 2011. Noble gas isotopes and the chemical composition of geothermal gases from the eastern part of the Büyük Menderes Graben (Turkey). J. Volcanol. Geoth. Res. 208 (3–4), 112–121. http://dx.doi.org/10.1016/j.jvolgeores.2011.09.009.

Wilcox, R.E., Harding, T.P., Seely, D.R., 1973. Basic Wrench Tectonics. Am. Assoc. Petrol. Geol. Bull. 57 (1), 74–96.

Yılmaz, Y., Genç, S.C., Gürer, Ö.F., Bozcu, M., Yılmaz, K., Karacık, Z., Altunkaynak, Ş., Elmas, A., 2000. When did the western Anatolian grabens begin to develop? In: Bozkurt, E., Winchester, J.A., Piper, J.D.A. (Eds.), Tectonics and Magmatism in Turkey and the Surrounding Area. Geological Society, London, Special Publications 173, pp. 353–384. http://dx.doi.org/10.1144/GSL.SP.2000.173.01.17.